DE GRUYTER Open Physics 2025; 23: 20250228

Research Article

Ibrahim Elbatal, Ehab M. Almetwally, Mohamed Kayid, Ahmed W. Shawki, Oluwafemi Samson Balogun, and Mohammed Elgarhy*

Sine power Burr X distribution with estimation and applications in physics and other fields

https://doi.org/10.1515/phys-2025-0228
received October 10, 2024; accepted October 01, 2025

Abstract: This article aims to introduce a new three-parameter lifetime distribution called sine power Burr X (SPB-X) distribution. The proposed distribution is obtained by the sine-G class of distributions and the power Burr X distribution. Various properties of the proposed distribution, including explicit expressions for the quantile function, Bowley skewness, Moors kurtosis, ordinary moments, generating function, incomplete and conditional moments, and some numerical and graphical illustrations, are provided. Some various significant reliability metrics for the SPB-X model, including common reliability functions, mean residual life function, mean waiting time function, residual moment, and reversed residual life. Several essential risk measures for the SPB-X distribution. These risk measures include the value at risk, the expected shortfall, the tail value at risk, the tail variance, and the tail variance premium. Four estimation methods were employed to estimate the model's parameters such as maximum likelihood, least squares, maximum product spacing, and Bayesian. A simulation study is conducted to assess the performance of the estimation methods. Finally, five real data are considered to analyze the usefulness and flexibility of the proposed model.

*** Corresponding author: Mohammed Elgarhy,** Department of Basic Sciences, Higher Institute of Administrative Sciences, Belbeis, AlSharkia, Egypt; Department of Computer Engineering, Biruni University, 34010, Istanbul, Turkey, e-mail: dr.moelgarhy@gmail.com
Ibrahim Elbatal: Department of Mathematics and Statistics, College of Science, Imam Mohammad Ibn Saud Islamic University (IMSIU), Riyadh 11432, Saudi Arabia, e-mail: iielbatal@imamu.edu.sa
Ehab M. Almetwally: Department of Mathematics and Statistics, College of Science, Imam Mohammad Ibn Saud Islamic University (IMSIU), Riyadh 11432, Saudi Arabia, e-mail: emalmetwally@imamu.edu.sa
Mohamed Kayid: Department of Statistics and Operations Research, College of Science, King Saud University, P.O. Box 2455, Riyadh 11451, Saudi Arabia, e-mail: drkayid@ksu.edu.sa
Ahmed W. Shawki: Central Agency for Public Mobilization & Statistics (CAPMAS), Cairo, Egypt, e-mail: ahmed23484@hotmail.com
Oluwafemi Samson Balogun: Department of Computing, University of Eastern Finland, FI-70211, Kuopio, Finland, e-mail: samson.balogun@uef.fi

Keywords: sine G family, power Burr-X distribution, actuarial measures, maximum likelihood estimation, Bayesian

1 Introduction

Recent years in the field of applied sciences have been characterized by the need and magnitude of data that require analysis. Recently, most statisticians have focused on developing new families that are a generalization of existing distributions to obtain a better fit for data modeling. These families of distributions are derived by compounding multiple distributions or incorporating additional parameters into the baseline model. Recent research has focused on the generation of families of distributions by authors. The beta-G family [1], Kumaraswamy-G [2], T-X family [3], Type II half logistic-G [4], and Topp-Leone odd Fréchet-G [5] are included in this classification. The families described by trigonometric transformations have garnered significant interest due to their applicability and effectiveness in various contexts. These families offer versatility and flexibility as the parameters fluctuate with changes in their values, while the periodic function governs the behavior of the distribution curve. The combination of diverse functions exhibiting distinct behaviors enhances the modeling of real-world phenomena, addressing the limitations of previously established generalized statistical distributions. The sine-G family of distributions, introduced in 2015, is recognized as the pioneering trigonometric family of distributions.

Another method of creating new life distributions by modifying trigonometric functions to produce new statistical distributions was introduced by Kumar *et al.* [6]. This generated family is called the sine G family and has the following cumulative distribution function (cdf) and probability density function (pdf) as follows:

$$F(x;\zeta) = \sin\left(\frac{\pi}{2}G(x,\zeta)\right), \quad x \in R \tag{1}$$

and

$$f(x;\zeta) = \frac{\pi}{2}g(x;\zeta)\cos\left(\frac{\pi}{2}G(x;\zeta)\right), \quad x \in R, \tag{2}$$

respectively, where $G(x,\zeta)$ and $g(x;\zeta)$ represent the cdf and pdf of the parent distribution, which has the parameter vector symbolized by ζ. This family offers several advantages, including the following. (1) It is simple. (2) The two cdfs $F(x)$ and $G(x)$ have the same number of parameters; there are no additional parameters, avoiding the problem of excessive parameterization. (3) The trigonometric function allows $F(x)$ to extend the flexibility of $G(x)$, resulting in new flexible models. Among the trigonometric families of distributions, a few of them, including Cos-G [7], sine Kumaraswamy-G [8], sine Topp-Leone-G [9], and Tan-G [10], arcsine exponentiated-X family [11], among others.

The Burr type X (B-X) distribution was first presented and examined by Burr [12]. The B-X distribution has widespread use in dependability research, agriculture, biology, and medicine. In addition, it can accurately depict mechanical strength data and overall lifespan statistics. Several researchers have examined the B-X distribution, starting with [13], which explored several features of the two-parameter B-X distribution and their relationship with other distributions. The beta B-X was examined by Surles and Padgett [14]. Algarni *et al.* [15] proposed the family of distributions formed by type I half-logistic B-X, whereas Abonongo *et al.* [16] discussed cosine Fréchet loss distribution, whereas Bantan *et al.* [17] presented the family of distributions generated by the truncated B-X. Suleiman *et al.* [18] studied new odd beta prime-B-X distribution, new truncated Zubair-generalized family studied by Soliman *et al.* [19] transmuted B-X distribution studied by Khan *et al.* [20], Topp-Leone Weibull generated family studied by Elbatal *et al.* [21] odd Burr-B-X distribution studied by Butt and Khalil [23], odd log-logistic B-X distribution studied by Usman *et al.* [24], type I half-logistic B-X distribution proposed by Shrahili *et al.* [25], Marshall-Olkin exponentiated B-X distribution investigated by Abdullah *et al.* [26], exponentiated generalized B-X distribution introduced by Khaleel *et al.* [27], beta Kumaraswamy B-X distribution presented by Madaki *et al.* [28], Weibull B-X distribution studied by Ishaq *et al.* [29], Marshall-Olkin extended B-X distribution investigated by Al-Saiari *et al.* [30], gamma B-X distribution introduced by Khaleel *et al.* [31], beta B-X distribution discussed by Merovci *et al.* [32], and Kavya-Manoharan-B-X distribution studied by Hassan *et al.* [33]. The cdf and pdf of the B-X distribution are provided *via*

$$G(x;\theta,\alpha) = [1 - e^{-(\theta x)^2}]^{\alpha}, \quad x > 0$$

and

$$g(x;\theta,\alpha) = 2\alpha\theta^2 x e^{-(\theta x)^2}[1 - e^{-(\theta x)^2}]^{\alpha-1},$$

where $\alpha > 0$ and $\theta > 0$ are the shape and scale parameters, respectively. By including a new parameter, the power transformation of a random variable can provide a more adaptable distribution model. The power B-X (PB-X) distribution was constructed in Ref. [22], with an additional shape parameter λ depending on the transformation procedure. The cdf and pdf of the PB-X distribution are provided and presented by

$$G(x;\theta,\lambda,\alpha) = [1 - e^{-(\theta x^{\lambda})^2}]^{\alpha}, \quad x > 0 \tag{3}$$

and

$$g(x;\theta,\lambda,\alpha) = 2\alpha\lambda\theta^2 x^{2\lambda-1} e^{-(\theta x^{\lambda})^2}[1 - e^{-(\theta x^{\lambda})^2}]^{\alpha-1}. \tag{4}$$

Often, the PB-X distribution is not flexible enough to represent a variety of lifetime data well. To address this limitation, we propose a novel extension of the PB-X distribution. Inspired by the sine-G family, the new suggested distribution is called the sine PB-X (SPB-X) distribution, and it has the same number of parameters as for the PB-X distribution. In this study, the following objectives will be the main focus:

1) Create a flexible distribution that can represent ft-skewed, right-skewed, decreased, unimodal, heavy-tailed, and closely to symmetric can be seen in its pdf. A variety of shapes, such as increasing, J-shaped, and decreasing patterns, can be seen in its hrf.
2) Compute some important statistical properties of the suggested distribution, including its quantile function (QF), Bowley skewness, Moors kurtosis, ordinary moments, generating function, incomplete and conditional moments, and some numerical and graphical illustrations.
3) Some significant reliability metrics are calculated for the SPB-X model, including common reliability functions, mean residual life function, mean waiting time function, residual moment, and reversed residual life.
4) Several essential risk measures include the value at risk, the expected shortfall (ES), the tail value at risk (TVaR), the tail variance (TV), and the tail variance premium (TVP).
5) Estimate the unknown parameters of the SPB-X distribution using four estimation methods, including maximum likelihood, least squares, maximum product spacing (MPS), and Bayesian. To evaluate the efficacy of these estimators in varying scenarios, perform a detailed simulation study.
6) As a result of its adaptability, the SPB-X distribution appears to be a good contender for modeling five datasets taken from the real world in contrast to other alternatives that are currently available. To illustrate its

superiority, this present article examines a variety of modern statistical models, such as the PB-X, shifting exponential Weibull exponential (SEWHE), Weibull, gamma, exponentiated Weibull, sine exponentiated Weibull exponential (SEWE) and Burr III (BIII) distributions.

In this study, an idea for an extension of the PB-X model is presented. The sine-G family serves as a framework for its construction, and the distribution is referred to as the sine power Burr X (SPB-X) distribution. The subsequent sections of this work are structured as follows. In Section 2, we present the SPB-X distribution and give visual representations of its density function. Section 3 examines the many statistical and mathematical features. Multiple reliability metrics are established in Section 4. Some theoretical and numerical actuarial measures are discussed in Section 5. Several different methods of estimation for the unknown parameters are derived in Section 6. A comprehensive Monte Carlo simulation investigation is conducted in Section 7. The utility of the SPB-X distribution is shown through the analysis of five actual datasets in Section 8. Ultimately, the conclusions are presented in Section 9.

2 Construction of the SPB-X model

In this article, we combine the sine G family and the PB-X distribution by inserting (3) in (1) to obtain the cdf of the SPB-X distribution as follows:

$$F_{\text{SPB-X}}(x;\theta,\lambda,\alpha) = \sin\left(\frac{\pi}{2}[1 - e^{-(\theta x^{\lambda})^2}]^{\alpha}\right), \tag{5}$$

where $x > 0$, $\theta, \lambda, \alpha > 0$. The corresponding pdf of the SPB-X distribution can be constructed by inserting (3) and (4) into (2) as follows:

$$\begin{aligned} &f_{\text{SPB-X}}(x;\theta,\lambda,\alpha) \\ &\quad= \frac{\pi}{2}2\alpha\lambda\theta^2 x^{2\lambda-1}e^{-(\theta x^{\lambda})^2}[1 - e^{-(\theta x^{\lambda})^2}]^{\alpha-1}\cos \\ &\quad\times\left(\frac{\pi}{2}[1 - e^{-(\theta x^{\lambda})^2}]^{\alpha}\right). \end{aligned} \tag{6}$$

Figure 1 illustrates some pdf curves for the SPB-X distribution at $\theta = 0.5$ (left panel) and $\theta = 1.5$ (right panel) and for different numerical values of α and λ. From Figure 1, we can note that the pdf for the SPB-X distribution can be left-skewed, right-skewed, decreased, unimodal, and closely symmetric shapes.

To obtain the explicit expression of the distribution, we use the generalized binomial theorem and the Taylor series expansion of the cosine function,

$$\cos\left[\frac{\pi}{2}G(x)\right] = \sum_{i=0}^{\infty}\frac{(-1)^i}{(2i)!}\left(\frac{\pi}{2}G(x)\right)^{2i} \tag{7}$$

and

$$(1 - z)^{b-1} = \sum_{i=0}^{\infty}(-1)^i\binom{b-1}{i}z^i. \tag{8}$$

By using (7) and (8), we have

$$\cos\left(\frac{\pi}{2}[1 - e^{-(\theta x^{\lambda})^2}]^{\alpha}\right) = \sum_{i=0}^{\infty}\frac{(-1)^i}{(2i)!}\left(\frac{\pi}{2}\right)^{2i}[1 - e^{-(\theta x^{\lambda})^2}]^{2\alpha i}.$$

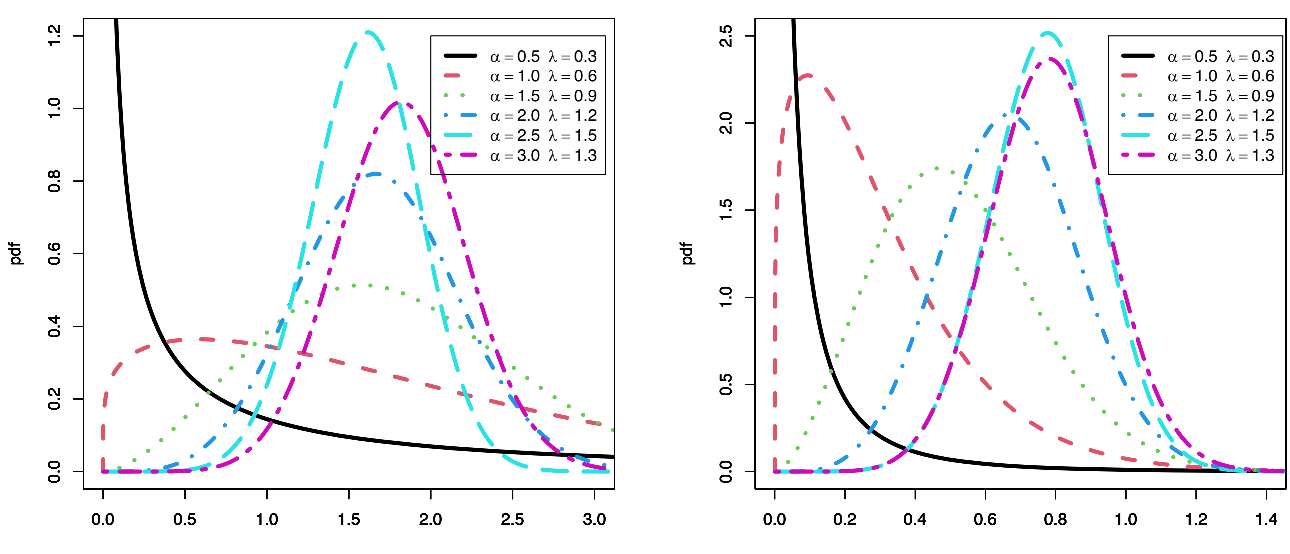

Figure 1: Plots of the pdf for the SPB-X distribution at $\theta = 0.5$ (left panel) and $\theta = 1.5$ (right panel).

One possible way to express the expansion of pdf in Eq. (6) is as follows:

$$f_{\text{SPB-X}}(x;\theta,\lambda,\alpha) = 2\alpha\lambda\theta^2 \sum_{i,j=0}^{\infty} \varphi^{(i,j)} x^{2\lambda-1} e^{-(j+1)(\theta x^{\lambda})^2}, \quad (9)$$

where

$$\varphi^{(i,j)} = \frac{(-1)^{i+j}}{(2i)!}\left(\frac{\pi}{2}\right)^{2i+1}\binom{(2i+1)\alpha-1}{j}.$$

3 Statistical and mathematical properties of SPB-X model

Several significant statistical and mathematical metrics for the SPB-X model are presented in this section.

3.1 Quantile function

There are several uses for the QF, including statistical applications, Monte Carlo techniques, and theoretical parts. The QF algorithm is used in Monte Carlo simulations to generate simulated random variables for classical and novel continuous distributions. It is possible to derive the pth QF of the SPB-X distribution by inverting the Eq. (5) as follows:

$$x_p = Q(p) = \left[-\frac{1}{\theta^2}\log\left(1-\left[\frac{2}{\pi}\arcsin(p)\right]^{\frac{1}{\alpha}}\right)\right]^{\frac{1}{2\lambda}}, \quad (10)$$

$p \in (0,1)$.

Bowley skewness, which was defined in [34], is considered one of the early skewness measurements that was offered as

$$\text{SK} = \frac{Q\left(\frac{3}{4}\right) + Q\left(\frac{1}{4}\right) - 2Q\left(\frac{1}{2}\right)}{Q\left(\frac{3}{4}\right) - Q\left(\frac{1}{4}\right)}.$$

As an alternative, Moors kurtosis [35], which is derived from quantiles, is presented by the following equation:

$$\text{KU} = \frac{Q\left(\frac{7}{8}\right) - Q\left(\frac{5}{8}\right) + Q\left(\frac{3}{8}\right) - Q\left(\frac{1}{8}\right)}{Q\left(\frac{6}{8}\right) - Q\left(\frac{2}{8}\right)}.$$

where $Q(\cdot)$ represents the QF.

Table 1 displays the values of $Q\left(\frac{1}{4}\right)$, $Q\left(\frac{1}{2}\right)$, and $Q\left(\frac{3}{4}\right)$, which represent the first, second (median), and third percentiles, respectively, offering valuable information on the distribution characteristics of the SPB-X model. The skewness (SK) coefficient quantifies the asymmetry of the distribution, while the kurtosis (KU) coefficient describes its peakedness relative to a normal distribution. These measures are provided for different values of the shape

Table 1: Results of $Q\left(\frac{1}{4}\right)$, $Q\left(\frac{1}{2}\right)$, $Q\left(\frac{3}{4}\right)$, SK, and KU associated with the SPB-X distribution when $\theta = 1.5$

λ	α	$Q\left(\frac{1}{4}\right)$	$Q\left(\frac{1}{2}\right)$	$Q\left(\frac{3}{4}\right)$	SK	KU
0.5	1.5	0.1559	0.2913	0.4835	0.1733	1.2573
	1.8	0.2000	0.3482	0.5502	0.1537	1.2532
	2.0	0.2278	0.3828	0.5899	0.1441	1.2517
	2.2	0.2544	0.4150	0.6263	0.1363	1.2507
	2.4	0.2797	0.4451	0.6600	0.1300	1.2504
	2.6	0.3038	0.4734	0.6914	0.1246	1.2498
	2.8	0.3268	0.5002	0.7207	0.1198	1.2497
	3.0	0.3489	0.5254	0.7482	0.1160	1.2497
	3.2	0.3699	0.5492	0.7741	0.1126	1.2496
	3.4	0.3901	0.5720	0.7987	0.1096	1.2496
	3.6	0.4094	0.5936	0.8219	0.1069	1.2497
	3.8	0.4280	0.6142	0.8440	0.1045	1.2497
	4.0	0.4459	0.6340	0.8650	0.1024	1.2498
1.6	1.5	0.5594	0.6801	0.7968	−0.0171	1.2289
	1.8	0.6047	0.7191	0.8297	−0.0172	1.2325
	2.0	0.6299	0.7407	0.8479	−0.0168	1.2340
	2.2	0.6520	0.7597	0.8640	−0.0165	1.2355
	2.4	0.6716	0.7765	0.8782	−0.0157	1.2364
	2.6	0.6891	0.7916	0.8911	−0.0151	1.2373
	2.8	0.7051	0.8053	0.9027	−0.0142	1.2380
	3.0	0.7196	0.8178	0.9133	−0.0140	1.2383
	3.2	0.7329	0.8293	0.9231	−0.0132	1.2391
	3.4	0.7451	0.8398	0.9321	−0.0126	1.2391
	3.6	0.7565	0.8496	0.9406	−0.0117	1.2393
	3.8	0.7670	0.8587	0.9484	−0.0112	1.2395
	4.0	0.7769	0.8673	0.9557	−0.0107	1.2399
2.5	1.5	0.6895	0.7814	0.8647	−0.0488	1.2418
	1.8	0.7248	0.8098	0.8874	−0.0454	1.2429
	2.0	0.7439	0.8252	0.8998	−0.0434	1.2437
	2.2	0.7605	0.8387	0.9107	−0.0415	1.2442
	2.4	0.7751	0.8505	0.9203	−0.0398	1.2442
	2.6	0.7880	0.8611	0.9288	−0.0382	1.2443
	2.8	0.7996	0.8706	0.9366	−0.0365	1.2446
	3.0	0.8101	0.8792	0.9436	−0.0353	1.2442
	3.2	0.8196	0.8871	0.9501	−0.0338	1.2444
	3.4	0.8284	0.8943	0.9560	−0.0327	1.2451
	3.6	0.8364	0.9009	0.9615	−0.0309	1.2441
	3.8	0.8439	0.9071	0.9667	−0.0302	1.2438
	4.0	0.8508	0.9129	0.9714	−0.0291	1.2441

parameters λ and α, with θ fixed at 1.5. Table 1 illustrates how variations in α and λ influence the distribution. Increasing these parameters results in a broader data spread, as reflected in higher percentile values. The skewness and kurtosis values highlight the model's flexibility in capturing different distributional shapes, making it adaptable to diverse real-world applications. These findings suggest that by adjusting λ and α, the SPB-X distribution can be tailored to exhibit varying degrees of skewness and symmetry, depending on the specific requirements of the dataset.

3.2 Moments and generating functions

The rth moment of the SPB-X model is calculated as follows:

$$\mu_r' = \int_0^\infty x^r f(x)\mathrm{d}x = 2\alpha\lambda\theta^2 \sum_{i,j=0}^{\infty} \varphi^{(i,j)} \int_0^\infty x^{r+2\lambda-1} e^{-(j+1)(\theta x^\lambda)^2}\mathrm{d}x.$$

By letting $y = (j+1)(\theta x^\lambda)^2$, after some algebra, the rth moment is provided *via*

$$\mu_r' = \frac{\alpha}{\theta^{\frac{r}{\lambda}}} \sum_{i,j=0}^{\infty} \varphi^{(i,j)} \frac{\Gamma(1+\frac{r}{2\lambda})}{(j+1)^{1+\frac{r}{2\lambda}}}. \tag{11}$$

The moment generating function of the SPB-X distribution may be defined as follows:

$$M_X(t) = \frac{\alpha}{\theta^{\frac{r}{\lambda}}} \sum_{i,j=0}^{\infty} \varphi^{(i,j)} \frac{t^r}{r!} \frac{\Gamma(1+\frac{r}{2\lambda})}{(j+1)^{1+\frac{r}{2\lambda}}}.$$

Table 2 presents the numerical values of the first four moments (μ_1', μ_2', μ_3', and μ_4'), along with variance (σ^2), standard deviation (σ), skewness (SK), kurtosis (KU), and coefficient of variation (CV) for the SPB-X distribution when $\theta = 1.5$. Table 2 illustrates the effect of varying the shape parameters λ and α on the distribution characteristics. As α increases for a fixed λ, both the mean and variance increase, indicating a wider spread of the distribution. SK values reveal how the distribution deviates from symmetry, transitioning between positive and negative values, demonstrating the model's ability to represent different distribution shapes, symmetric or skewed to the left or right.

Furthermore, the values of KU indicate the degree of peakness in the distribution. Higher values correspond to a leptokurtic distribution (more peaked), whereas lower values suggest a platykurtic distribution (flatter). CV reflects the relative dispersion of the data around the mean, with lower values indicating greater homogeneity and higher values suggesting greater variability.

In general, these results highlight the flexibility of the SPB-X distribution and its ability to be customized for different applications by adjusting the shape parameters λ and α to fit the characteristics of the data under analysis. Figure 2 shows 3D plots of the moments measurements for the SPB-X distribution at $\theta = 2.5$.

3.3 Incomplete moments

The sth incomplete moment of the SPB-X distribution is given by

$$\begin{aligned} m_s(t) = E(X^s|X<t) &= \int_0^t x^s f(x)\mathrm{d}x \\ &= 2\alpha\lambda\theta^2 \sum_{i,j=0}^{\infty} \varphi^{(i,j)} \int_0^t x^{s+2\lambda-1} e^{-(j+1)(\theta x^\lambda)^2}\mathrm{d}x \\ &= \frac{\alpha}{\theta^{\frac{s}{\lambda}}} \sum_{i,j=0}^{\infty} \varphi^{(i,j)} \frac{\gamma(1+\frac{s}{2\lambda}, (j+1)(\theta t^\lambda)^2)}{(j+1)^{1+\frac{s}{2\lambda}}}, \end{aligned} \tag{12}$$

where $\gamma(s,t) = \int_0^t x^{s-1}e^{-x}\mathrm{d}x$ is the lower incomplete gamma function.

3.4 Conditional moments

For the SPB-X model, the conditional moments defined by $E(X^s|X>t)$. It can be written as follows:

$$E(X^s|X>t) = \frac{1}{\overline{F}(t)}\kappa_s(t),$$

where

$$\begin{aligned} \kappa_s(t) &= \int_t^\infty x^s f(x)\mathrm{d}x \\ &= 2\alpha\lambda\theta^2 \sum_{i,j=0}^{\infty} \varphi^{(i,j)} \int_t^\infty x^{s+2\lambda-1} e^{-(j+1)(\theta x^\lambda)^2}\mathrm{d}x \\ &= \frac{\alpha}{\theta^{\frac{s}{\lambda}}} \sum_{i,j=0}^{\infty} \varphi^{(i,j)} \frac{\Gamma(1+\frac{s}{2\lambda}, (j+1)(\theta t^\lambda)^2)}{(j+1)^{1+\frac{s}{2\lambda}}}, \end{aligned} \tag{13}$$

and $\Gamma(s,t) = \int_t^\infty x^{s-1}e^{-x}\mathrm{d}x$ is the upper incomplete gamma function.

4 Reliability measures

In this section, we suggested various significant reliability metrics for the SPB-X model, including common reliability functions, mean residual life function, mean waiting time function, residual moment, and reversed residual life.

4.1 Common reliability functions

The common reliability functions of SPB-X distribution are survival, hazard rate function (hrf), and reversed hrf, where the survival or reliability function is given by

$$\overline{F}(x) = 1 - \sin\left(\frac{\pi}{2}[1 - e^{-(\theta x^{\lambda})^2}]^{\alpha}\right).$$

The hrf is provided *via*

$$\tau(x) = \frac{f(x)}{\overline{F}(x)} = \frac{\pi}{2}2\alpha\lambda\theta^2 x^{2\lambda-1}e^{-(\theta x^{\lambda})^2}[1 - e^{-(\theta x^{\lambda})^2}]^{\alpha-1} \times \frac{\cos\left(\frac{\pi}{2}[1 - e^{-(\theta x^{\lambda})^2}]^{\alpha}\right)}{1 - \sin\left(\frac{\pi}{2}[1 - e^{-(\theta x^{\lambda})^2}]^{\alpha}\right)},$$

and reversed hrf is provided *via*

Table 2: Numerical outcomes for the first four moments, σ^2, σ, SK, KU, and CV for the SPB-X distribution when $\theta = 1.5$

λ	α	μ_1'	μ_2'	μ_3'	μ_4'	σ^2	σ	SK	KU	CV
0.5	1.5	0.3538	0.1973	0.1494	0.1432	0.0721	0.2685	1.4774	6.3418	0.7590
	1.8	0.4080	0.2462	0.1958	0.1939	0.0797	0.2823	1.3496	5.8230	0.6919
	2.0	0.4410	0.2784	0.2280	0.2301	0.0839	0.2897	1.2846	5.5792	0.6568
	2.2	0.4719	0.3102	0.2609	0.2681	0.0876	0.2959	1.2308	5.3877	0.6272
	2.4	0.5008	0.3416	0.2944	0.3077	0.0908	0.3013	1.1855	5.2339	0.6018
	2.6	0.5280	0.3724	0.3284	0.3486	0.0937	0.3061	1.1469	5.1080	0.5797
	2.8	0.5536	0.4027	0.3628	0.3908	0.0962	0.3102	1.1136	5.0031	0.5603
	3.0	0.5779	0.4325	0.3974	0.4342	0.0985	0.3139	1.0845	4.9147	0.5431
	3.2	0.6010	0.4618	0.4322	0.4786	0.1006	0.3171	1.0589	4.8391	0.5277
	3.4	0.6230	0.4905	0.4672	0.5239	0.1024	0.3201	1.0362	4.7739	0.5138
	3.6	0.6439	0.5187	0.5023	0.5701	0.1041	0.3227	1.0160	4.7172	0.5012
	3.8	0.6639	0.5465	0.5374	0.6170	0.1057	0.3251	0.9978	4.6673	0.4897
	4.0	0.6831	0.5737	0.5726	0.6646	0.1071	0.3273	0.9813	4.6233	0.4791
1.6	1.5	0.6771	0.4888	0.3716	0.2953	0.0302	0.1739	−0.0526	2.8624	0.2568
	1.8	0.7161	0.5402	0.4259	0.3488	0.0275	0.1658	−0.0674	2.9135	0.2315
	2.0	0.7377	0.5702	0.4587	0.3821	0.0260	0.1611	−0.0715	2.9387	0.2184
	2.2	0.7568	0.5974	0.4892	0.4137	0.0246	0.1570	−0.0726	2.9587	0.2074
	2.4	0.7738	0.6223	0.5176	0.4438	0.0235	0.1533	−0.0719	2.9748	0.1981
	2.6	0.7891	0.6451	0.5443	0.4725	0.0225	0.1499	−0.0700	2.9879	0.1900
	2.8	0.8029	0.6663	0.5694	0.4998	0.0216	0.1469	−0.0671	2.9987	0.1830
	3.0	0.8156	0.6859	0.5931	0.5261	0.0208	0.1442	−0.0637	3.0077	0.1768
	3.2	0.8272	0.7043	0.6156	0.5512	0.0201	0.1417	−0.0599	3.0153	0.1713
	3.4	0.8379	0.7215	0.6369	0.5753	0.0194	0.1394	−0.0559	3.0218	0.1663
	3.6	0.8478	0.7376	0.6572	0.5985	0.0188	0.1372	−0.0532	3.0391	0.1619
	3.8	0.8571	0.7529	0.6765	0.6209	0.0183	0.1352	−0.0475	3.0322	0.1578
	4.0	0.8657	0.7673	0.6950	0.6424	0.0178	0.1334	−0.0432	3.0364	0.1541
2.5	1.5	0.7728	0.6145	0.5007	0.4168	0.0172	0.1310	−0.3461	3.1244	0.1695
	1.8	0.8023	0.6585	0.5516	0.4705	0.0149	0.1220	−0.3347	3.1557	0.1520
	2.0	0.8184	0.6834	0.5812	0.5025	0.0137	0.1171	−0.3245	3.1657	0.1431
	2.2	0.8323	0.7055	0.6080	0.5319	0.0127	0.1128	−0.3135	3.1704	0.1356
	2.4	0.8446	0.7253	0.6324	0.5591	0.0119	0.1092	−0.3021	3.1719	0.1292
	2.6	0.8556	0.7433	0.6548	0.5844	0.0112	0.1059	−0.2908	3.1712	0.1238
	2.8	0.8655	0.7597	0.6755	0.6081	0.0106	0.1030	−0.2797	3.1691	0.1191
	3.0	0.8744	0.7747	0.6948	0.6303	0.0101	0.1005	−0.2690	3.1663	0.1149
	3.2	0.8826	0.7885	0.7127	0.6511	0.0096	0.0981	−0.2586	3.1630	0.1112
	3.4	0.8900	0.8014	0.7295	0.6708	0.0092	0.0960	−0.2486	3.1594	0.1079
	3.6	0.8969	0.8134	0.7452	0.6895	0.0089	0.0941	−0.2391	3.1557	0.1049
	3.8	0.9033	0.8246	0.7601	0.7072	0.0085	0.0923	−0.2300	3.1520	0.1022
	4.0	0.9093	0.8351	0.7741	0.7241	0.0082	0.0907	−0.2212	3.1484	0.0997

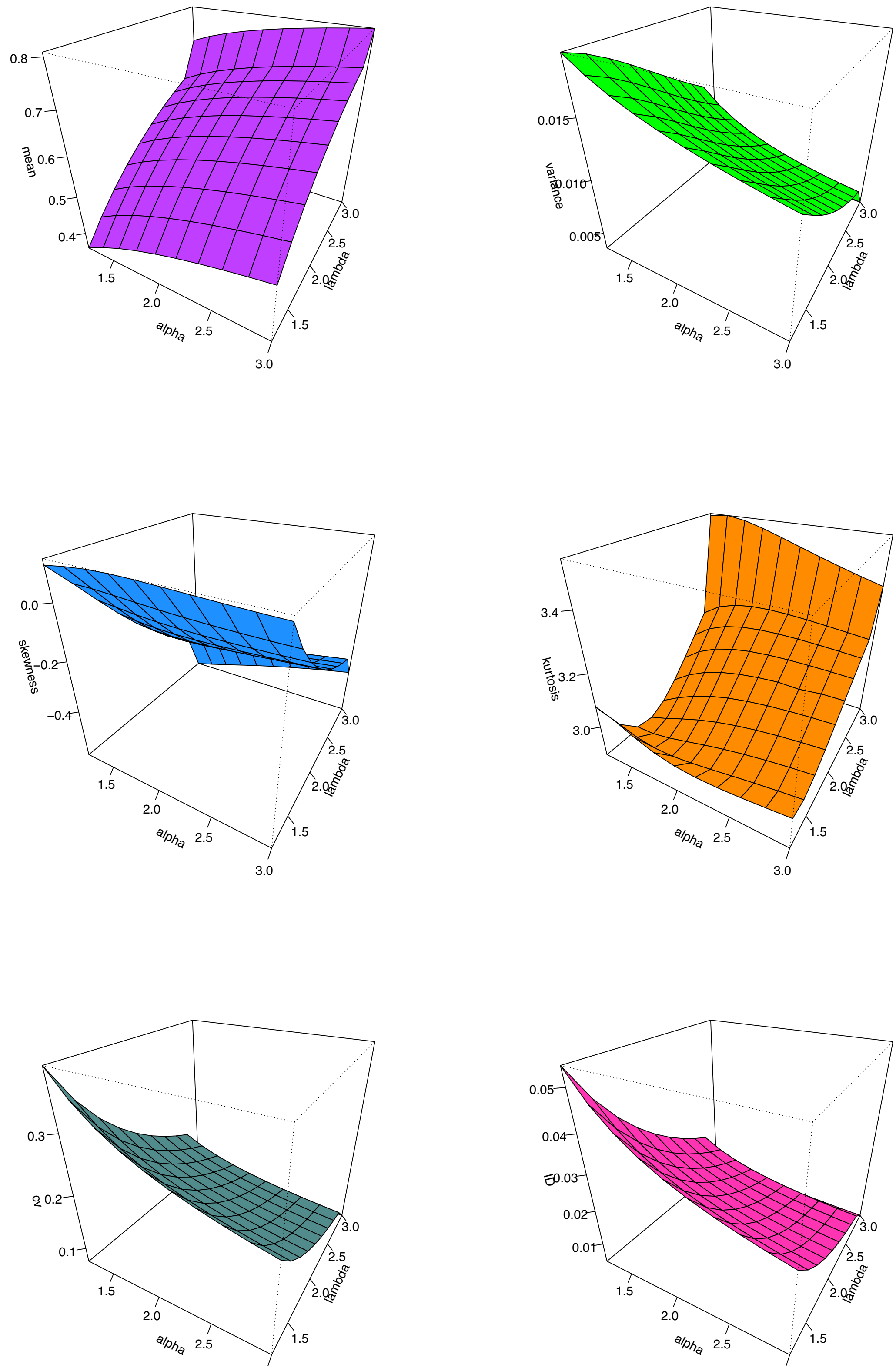

Figure 2: 3D plots of the moments measurements for the SPB-X distribution at $\theta = 2.5$.

$$\varsigma(x) = \frac{f(x)}{F(x)} = \frac{\pi}{2}2\alpha\lambda\theta^2 x^{2\lambda-1}e^{-(\theta x^\lambda)^2}[1 - e^{-(\theta x^\lambda)^2}]^{\alpha-1} \times \cot\left(\frac{\pi}{2}[1 - e^{-(\theta x^\lambda)^2}]^\alpha\right).$$

Figure 3 illustrates some hrf curves for the SPB-X distribution at $\theta = 0.5$ (left panel) and $\theta = 1.5$ (right panel) and for different numerical values of α and λ. From Figure 3, we can note that the hrf for the SPB-X distribution can be decreased, increased, and J-shaped.

4.2 Mean residual life function

To characterize lifespan distributions, the mean residual life (MRL) function is of critical significance in the fields of dependability, survival analysis, actuarial sciences, economics, and social sciences. In addition, it is an essential component in the repair and replacement methods and provides a comprehensive summary of the residual life function. The MRL function may be derived for the SPB-X distribution from the following:

$$\mu(t) = E((X-t)|X > t) = \left\{\frac{1}{\bar{F}(t)}\int_t^\infty xf \quad (x)\mathrm{d}x\right\} - t$$
$$= \frac{\alpha}{\bar{F}(t)\theta^{\frac{1}{\lambda}}}\sum_{i,j=0}^{\infty}\varphi^{(i,j)}\frac{\Gamma(1+\frac{1}{2\lambda}, (j+1)(\theta t^\lambda)^2)}{(j+1)^{1+\frac{1}{2\lambda}}} - t.$$

4.3 Mean inactivity time function

Given that $T_i \leqslant t$, the mean waiting time indicates the meantime that has passed since the T_i hazard. This is also known as the mean past lifetime (MPL). The random variable of interest in this case is $(t - T_i|T_i \le t)$, where $i = 1, 2, \ldots, n$. Given that T_i failed before t, this conditional random variable displays the time that has passed since the hazard. The average previous lifespan is provided by

$$\upsilon(t) = E(t - X|X \le t) = t - \frac{1}{F(t)}\int_0^t xf(x)\mathrm{d}x$$
$$= t - \frac{\alpha}{F(t)\theta^{\frac{1}{\lambda}}}\sum_{i,j=0}^{\infty}\varphi^{(i,j)}\frac{\gamma(1+\frac{1}{2\lambda}, (j+1)(\theta t^\lambda)^2)}{(j+1)^{1+\frac{1}{2\lambda}}}.$$

4.4 Moment of residual and reversed residual lifes

The residual life is the duration beyond t before failure occurs, specified by the conditional random variable $X - t|X > t$. The nth-order moment of the residual life of the random variable X is expressed as follows:

$$\varphi_n(t) = E((X-t)^n|X > t) = \frac{1}{\bar{F}(t)}\int_t^\infty (x-t)^n f(x)\mathrm{d}x, n \ge 1.$$

Employing (8) and utilizing the binomial expansion of $(x - t)^n$ in the aforementioned calculation yields

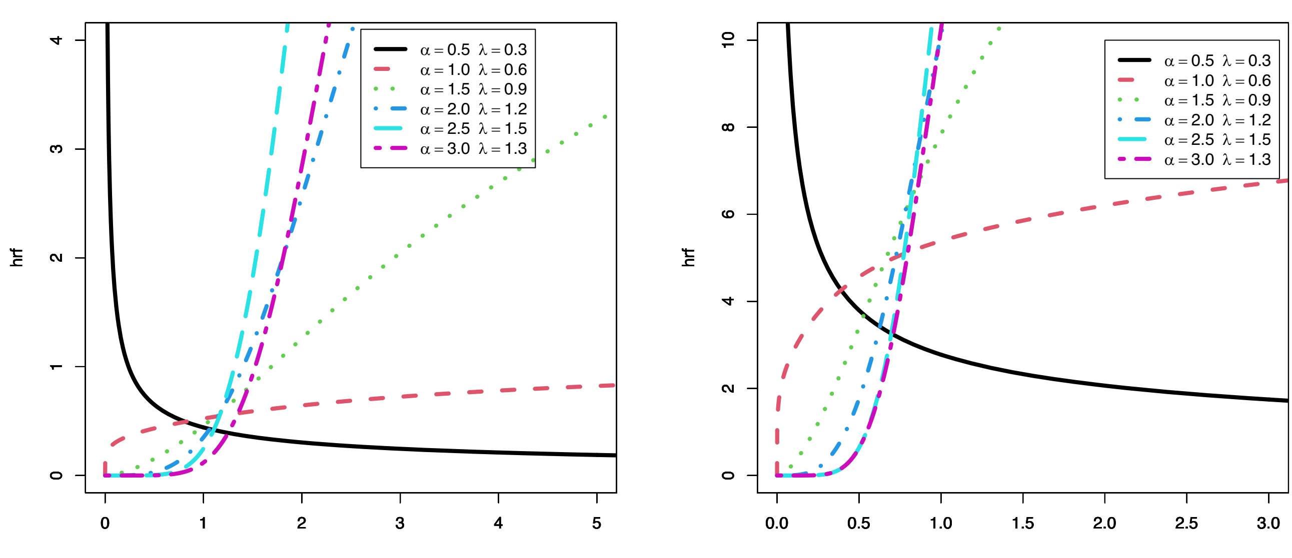

Figure 3: Plots of the hrf for the SPB-X distribution at $\theta = 0.5$ (left panel) and $\theta = 1.5$ (right panel).

$$\varphi_n(t) = \frac{1}{\overline{F}(t)} \sum_{d=0}^{n} (-t)^{n-d} \binom{n}{d} \int_t^\infty x^n f(x) \mathrm{d}x$$
$$= \frac{\alpha}{\overline{F}(t)\theta^{\frac{s}{\lambda}}} \sum_{i,j=0}^{\infty} \sum_{d=0}^{n} \varphi^{(i,j)} (-t)^{n-d} \binom{n}{d} \frac{\Gamma(1 + \frac{s}{2\lambda}, (j+1)(\theta t^\lambda)^2)}{(j+1)^{1+\frac{s}{2\lambda}}}.$$

On the other hand, the rth moment of the reversed residual life can be obtained by the following formula:

$$\xi_r(t) = E((t - X)^r | X \le t) = \frac{1}{F(t)} \int_0^t (t - x)^r f(x) \mathrm{d}x.$$

By utilizing (8) and employing the binomial expansion of $(t - x)^r$ in the aforementioned formula, we obtain

$$\xi_r(t) = \frac{1}{F(t)} \sum_{d=0}^{r} (-t)^{r-d} \binom{r}{d} \int_0^t x^r f(x) \mathrm{d}x = \frac{\alpha}{F(t)\theta^{\frac{s}{\lambda}}}$$
$$\times \sum_{i,j=0}^{\infty} \sum_{d=0}^{n} \varphi^{(i,j)} (-t)^{n-d} \binom{n}{d} \frac{\gamma(1 + \frac{s}{2\lambda}, (j+1)(\theta t^\lambda)^2)}{(j+1)^{1+\frac{s}{2\lambda}}}.$$

5 Actuarial measures

In actuarial practice, evaluating risk exposures is essential for companies. One of the primary goals of actuarial science institutes is to forecast market risks within a portfolio of instruments. Consequently, assessing risk measures is crucial in purchasing and selling products. In this section, we will explore many essential risk measures for the SPB-X distribution. These risk measures include the value at risk (VaR), the ES, the TVaR, the TV, and the TVP [47].

5.1 VaR measure

Risk managers often focus on the likelihood of an unfavorable result, which can be quantified using VaR at a certain probability level. The VaR [36] is used to assess risk exposure, thereby determining the capital required to endure undesirable outcomes. The VaR of the SPB-X distribution is specified as follows:

$$\mathrm{VaR}_q = \left[-\frac{1}{\theta^2} \log \left(1 - \left[\frac{2}{\pi} \arcsin(q) \right]^{\frac{1}{\alpha}} \right) \right]^{\frac{1}{2\lambda}}. \tag{14}$$

5.2 ES measure

Another significant financial metric is the ES, first articulated by [37,38]. The ES is a metric that provides superior justification for trading relative to VaR.

$$\mathrm{ES} = \frac{1}{q} \int_0^q \mathrm{VaR}_q \mathrm{d}x$$

for $0 < q < 1$ and VaR_q define in Eq. (4.1).

5.3 TVaR measure

The TVaR is a crucial risk metric. When an event occurs over a set probability threshold, TVaR is used to assess the expected value of the incurred loss. The TVaR of the SPB-X distribution is explicitly specified as follows:

$$\mathrm{TVaR}_q(x) = \frac{1}{1-q} \int_{\mathrm{VaR}_q}^{\infty} x f(x) \mathrm{d}x$$
$$= \frac{1}{1-q} \frac{\alpha}{\theta^{\frac{1}{\lambda}}} \sum_{i,j=0}^{\infty} \varphi^{(i,j)} \tag{15}$$
$$\times \frac{\Gamma(1 + \frac{1}{2\lambda}, (j+1)(\theta(\mathrm{VaR}_q))^\lambda)^2}{(j+1)^{1+\frac{1}{2\lambda}}}.$$

5.4 TV measure

The TV risk measure, as put up by Landsman [39], is summarized as the variance of the loss distribution above a certain critical threshold. The TV of the SPB-X distribution may be characterized as follows:

$$\mathrm{TV}_q(x) = E(X^2 | X > x_q) - (\mathrm{TVaR}_q)^2, \tag{16}$$

where

$$E(X^2 | X > x_q) = \frac{1}{1-q} \int_{\mathrm{VaR}_q}^{\infty} x^2 f(x) \mathrm{d}x$$
$$= \frac{1}{1-q} \frac{\alpha}{\theta^{\frac{2}{\lambda}}} \sum_{i,j=0}^{\infty} \varphi^{(i,j)} \tag{17}$$
$$\times \frac{\Gamma(1 + \frac{1}{\lambda}, (j+1)(\theta(\mathrm{VaR}_q))^\lambda)^2}{(j+1)^{1+\frac{1}{\lambda}}}.$$

5.5 TVP measure

The TVP is another important measure that plays an essential role in insurance sciences and is the mixture of central tendency and dispersion statistics. The TVP of SPB-X distribution takes the following form:

$$\mathrm{TV\,P}_q(x) = \mathrm{TVaR}_q + \omega \mathrm{TV}_q(x), \tag{18}$$

where $0 < \omega < 1$.

Key actuarial metrics, such as VaR, ES, Tail TVaR, TV, and TVP, are summarized in Table 3 for various combinations of λ and α at a fixed $\theta = 1.5$. Both VaR and ES increase when the quantile level (q) increases from 0.650 to 0.995, indicating higher risks at higher confidence levels. TVaR captures more risk in the tail by also following this increasing trend. Meanwhile, TV exhibits constancy in severe loss distributions and stays constant across circumstances. As q and ω grow, TVP measurements reveal increasing contributions from the tail, with $\omega = 0.9$ indicating the largest influence.

6 Estimation methods

6.1 Maximum likelihood estimation (MLE)

The MLEs [45,58] is the most widely used method of parameter estimation. Let $x_1, x_2, \ldots, x_n$ be a random sample (RS) of size n from the SPB-X distribution; then the log-likelihood function without constant term is given by

Table 3: Actuarial measures for $\theta = 1.5$

λ	α	q	VaR	ES	TVaR	TV	TVP		
							$\omega = 0.5$	$\omega = 0.75$	$\omega = 0.9$
0.5	0.5	0.650	0.1008	0.0298	0.2774	0.0375	0.2961	0.3055	0.3112
		0.700	0.1241	0.0357	0.3049	0.0385	0.3242	0.3338	0.3395
		0.750	0.1531	0.0425	0.3383	0.0395	0.3580	0.3679	0.3738
		0.800	0.1904	0.0505	0.3801	0.0405	0.4004	0.4105	0.4166
		0.850	0.2408	0.0601	0.4354	0.0417	0.4563	0.4668	0.4730
		0.900	0.3154	0.0721	0.5155	0.0432	0.5371	0.5479	0.5544
		0.950	0.4498	0.0880	0.6567	0.0450	0.6792	0.6904	0.6972
		0.975	0.5903	0.0989	0.8018	0.0463	0.8250	0.8365	0.8435
		0.990	0.7821	0.1075	0.9976	0.0474	1.0213	1.0332	1.0403
		0.995	0.9302	0.1113	1.1476	0.0481	1.1717	1.1837	1.1909
	1.2	0.650	0.3211	0.1485	0.5605	0.0536	0.5873	0.6008	0.6088
		0.700	0.3601	0.1622	0.5972	0.0531	0.6238	0.6371	0.6450
		0.750	0.4054	0.1768	0.6403	0.0526	0.6666	0.6797	0.6876
		0.800	0.4597	0.1928	0.6924	0.0521	0.7185	0.7315	0.7393
		0.850	0.5285	0.2104	0.7590	0.0516	0.7848	0.7977	0.8055
		0.900	0.6237	0.2305	0.8521	0.0510	0.8776	0.8903	0.8980
		0.950	0.7835	0.2550	1.0094	0.0504	1.0346	1.0472	1.0548
		0.975	0.9409	0.2703	1.1656	0.0499	1.1906	1.2031	1.2106
		0.990	1.1473	0.2818	1.3708	0.0498	1.3957	1.4082	1.4156
		0.995	1.3025	0.2865	1.5257	0.0496	1.5505	1.5629	1.5703
1.6	0.5	0.650	0.4882	0.2854	0.6440	0.0146	0.6513	0.6549	0.6571
		0.700	0.5210	0.3010	0.6672	0.0133	0.6738	0.6772	0.6792
		0.750	0.5564	0.3169	0.6929	0.0120	0.6989	0.7019	0.7037
		0.800	0.5956	0.3330	0.7223	0.0107	0.7276	0.7303	0.7319
		0.850	0.6409	0.3498	0.7571	0.0093	0.7618	0.7641	0.7655
		0.900	0.6973	0.3674	0.8018	0.0078	0.8057	0.8077	0.8089
		0.950	0.7791	0.3868	0.8689	0.0060	0.8719	0.8735	0.8744
		0.975	0.8482	0.3976	0.9272	0.0050	0.9297	0.9309	0.9317
		0.990	0.9261	0.4050	0.9946	0.0042	0.9967	0.9977	0.9983
		0.995	0.9776	0.4077	1.0409	0.0028	1.0423	1.0430	1.0434
	1.2	0.650	0.7012	0.5220	0.8222	0.0089	0.8266	0.8289	0.8302
		0.700	0.7268	0.5357	0.8402	0.0082	0.8443	0.8463	0.8475
		0.750	0.7541	0.5493	0.8601	0.0074	0.8638	0.8657	0.8668
		0.800	0.7844	0.5631	0.8830	0.0066	0.8863	0.8879	0.8889
		0.850	0.8193	0.5771	0.9102	0.0058	0.9131	0.9145	0.9154
		0.900	0.8629	0.5917	0.9451	0.0051	0.9476	0.9489	0.9497
		0.950	0.9266	0.6075	0.9985	0.0039	1.0004	1.0014	1.0020
		0.975	0.9812	0.6163	1.0455	0.0032	1.0471	1.0480	1.0484
		0.990	1.0439	0.6222	1.1008	0.0027	1.1022	1.1028	1.1033
		0.995	1.0861	0.6245	1.1384	0.0028	1.1398	1.1405	1.1409

$$
\begin{aligned}
L = {} & n\log(\alpha) + n\log(\lambda) + 2n\log(\theta) \\
& + (2\lambda - 1)\sum_{i=1}^{n}\log(x_i) \\
& - \theta^2\sum_{i=1}^{n}x_i^{2\lambda} + (\alpha - 1)\sum_{i=1}^{n}\log(1 - e^{-(\theta x^{\lambda})^2}) \\
& + \sum_{i=1}^{n}\log\left[\cos\left(\frac{\pi}{2}[1 - e^{-(\theta x^{\lambda})^2}]^{\alpha}\right)\right].
\end{aligned} \tag{19}
$$

To obtain the MLEs of parameters, we differentiate (19) partially with respect to θ, λ, and α and equating them to zero, we obtain the following three equations:

$$
\begin{aligned}
\frac{\partial L}{\partial\theta} = {} & \frac{2n}{\theta} + 2\sum_{i=1}^{n}\log(x_i) - 2\theta\sum_{i=1}^{n}x_i^{2\lambda} \\
& + 2\theta(\alpha - 1)\sum_{i=1}^{n}\frac{x_i^{2\lambda}e^{-(\theta x_i^{\lambda})^2}}{1 - e^{-(\theta x^{\lambda})^2}} \\
& + \sum_{i=1}^{n}\frac{\pi\theta\alpha x_i^{2\lambda}e^{-(\theta x_i^{\lambda})^2}\tan\left(\frac{\pi}{2}[1 - e^{-(\theta x^{\lambda})^2}]^{\alpha}\right)}{[1 - e^{-(\theta x^{\lambda})^2}]^{1-\alpha}},
\end{aligned} \tag{20}
$$

$$
\begin{aligned}
\frac{\partial L}{\partial\lambda} = {} & \frac{n}{\lambda} + 2\sum_{i=1}^{n}\log(x_i) - 2\theta^2\sum_{i=1}^{n}\log(x_i)x_i^{2\lambda} \\
& + (\alpha - 1)\sum_{i=1}^{n}\frac{\log(x_i)x_i^{2\lambda}e^{-(\theta x^{\lambda})^2}}{1 - e^{-(\theta x^{\lambda})^2}} \\
& + \theta^2\sum_{i=1}^{n}\frac{\pi x_i^{2\lambda}\log(x_i)\tan\left(\frac{\pi}{2}[1 - e^{-(\theta x^{\lambda})^2}]^{\alpha}\right)}{e^{(\theta x_i^{\lambda})^2}[1 - e^{-(\theta x^{\lambda})^2}]^{1-\alpha}},
\end{aligned} \tag{21}
$$

and

$$
\begin{aligned}
\frac{\partial L}{\partial\alpha} = {} & \frac{n}{\alpha} + \sum_{i=1}^{n}\log(1 - e^{-(\theta x^{\lambda})^2}) \\
& + \sum_{i=1}^{n}\frac{\pi\log(1 - e^{-(\theta x^{\lambda})^2})\tan\left(\frac{\pi}{2}[1 - e^{-(\theta x^{\lambda})^2}]^{\alpha}\right)}{2[1 - e^{-(\theta x^{\lambda})^2}]^{-\alpha}}.
\end{aligned} \tag{22}
$$

Then the maximum likelihood estimates of the parameters θ, λ, and α denoted by $\hat{\theta}, \hat{\lambda}$, and $\hat{\alpha}$, respectively, are obtained by solving the aforementioned three equations simultaneously.

6.2 Least squares estimators (LSEs)

The LSEs [46,48,49] are key in regression and estimation analysis, with the aim of minimizing the squared differences between observed and predicted values. In linear regression, LSE finds the coefficients that best fit the data. For a RS $x_{(1)} < x_{(2)} < \cdots < x_{(n)}$ from the SPB-X distribution, the LSE for α, θ, and λ minimizes an objective function to achieve the best data fit.More precisely, the LSE minimizes the following objective function:

$$
\mathrm{LSE} = \sum_{i=1}^{n}\left(\frac{i}{n} - \sin\left(\frac{\pi}{2}[1 - e^{-(\theta x^{\lambda})^2}]^{\alpha}\right)\right)^2.
$$

This minimization aims to identify the optimal values of α, θ, and λ, yielding estimates that align the empirical cumulative distribution function with the theoretical one based on the ordered sample, resulting in the best possible fit to the data.

6.3 MPS

MPS estimators are vital in statistical inference, offering efficient parameter estimates for probability distributions, especially useful in survival analysis and reliability modeling with censored data. In survival analysis, where not all failure times in a sample are fully observed, MPS estimators effectively manage such censoring. The method involves MPS between observed failure times to estimate distribution parameters. These estimators are recognized for their robustness against outliers and their strong performance across various distributional assumptions. MPS estimators are widely used in different fields. Further discussions on MPS can be found in papers by previous studies [43,44, 50,51].

The MPS estimators for θ and λ are derived by minimizing the following expression:

$$
D_i = F(x_i; \theta, \lambda, \alpha) - F(x_{i-1}; \theta, \lambda, \alpha); \quad i = 1, \ldots, n + 1,
$$

where $\sum D_i = 1$, then the natural logarithm of product spacing function of SPB-X distribution is

$$
\begin{aligned}
\mathrm{MPS} = \frac{1}{n + 1}\sum_{i=1}^{n+1}\ln\Bigg[& \sin\left(\frac{\pi}{2}[1 - e^{-(\theta x_{(i)}^{\lambda})^2}]^{\alpha}\right) \\
& - \sin\left(\frac{\pi}{2}[1 - e^{-(\theta x_{(i-1)}^{\lambda})^2}]^{\alpha}\right)\Bigg].
\end{aligned}
$$

6.4 Bayesian estimation

In this subsection, we utilize the Bayesian estimation method to estimate the unknown parameters of the SPB-X distribution. The core concept of the Bayesian approach is that the model's parameters are treated as random variables with a predefined distribution, known as the prior distribution. When prior knowledge is available, selecting an appropriate prior is essential. We choose the gamma conjugate prior for the parameters due to several reasons, such as its flexibility, noninformative nature, and the simplicity, it offers in analytical or computational updates to the posterior. In addition, its positive domain makes it well suited for modeling parameters. We implement the Bayesian inference method to estimate the unknown parameters $\Theta = (\theta, \lambda, \alpha)$. We assume independent gamma priors for θ, λ, and α. Specifically, θ, λ, and α follow a Gamma distribution $\Gamma(c_i, d_i)$, where c_i and d_i are positive hyperparameters for $i = 1, 2, 3$.

The estimates have been derived using the square error loss function. Therefore, the joint prior density of the independent parameters is expressed as follows:

$$\pi(\Theta) = \pi(\theta)\pi(\lambda)\pi(\alpha)$$

and

$$\pi(\Theta) = \theta^{c_1-1}e^{-d_1\theta}\lambda^{c_2-1}e^{-d_2\lambda}\alpha^{c_3-1}e^{-d_3\alpha}, \tag{23}$$

where $\theta > 0, \lambda > 0, \alpha > 0$. The joint posterior for the parameters can be obtained by incorporating the observed censored samples along with the prior distributions of these parameters, as shown below:

$$\begin{aligned}\pi^*(\Theta, x) = \pi(\Theta)L(\Theta|x) &\propto \theta^{2n+c_1-1}e^{-d_1\theta}\lambda^{n+c_2-1} \\ &\times e^{-d_2\lambda}\alpha^{n+c_3-1}e^{-d_3\alpha}e^{-\sum_{i=1}^{n}(\theta x_i^{\lambda})^2} \\ &\times \prod_{i=1}^{r}\frac{x_i^{2\lambda-1}\cos\left(\frac{\pi}{2}[1-e^{-(\theta x_i^{\lambda})^2}]^{\alpha}\right)}{[1-e^{-(\theta x_i^{\lambda})^2}]^{1-\alpha}}.\end{aligned} \tag{24}$$

Table 4: RAB, RMSE, and ranked of estimation methods for parameters of SPB-X distribution

$\theta = 0.5, \lambda = 0.75$			MLE				LS				MPS				Bayeaisan			
α	n		RAB		RMSE		RAB		RMSE		RAB		RMSE		RAB		RMSE	
1.5	25	α	0.098349	1	0.535404	1	0.008759	4	0.16359	4	0.028028	3	0.525338	2	0.096516	2	0.497735	3
		θ	0.087211	1	0.159227	1	−0.05332	4	0.083594	4	0.086144	2	0.14988	2	0.03257	3	0.12008	3
		λ	0.014938	3	0.212967	1	0.006078	4	0.130798	4	0.018591	2	0.186292	2	0.063172	1	0.142277	3
		∑ Rank	5		3		12		12		7		6		6		9	
	70	α	0.064606	2	0.517576	1	0.004599	4	0.099651	4	0.01644	3	0.325084	3	0.085276	1	0.398442	2
		θ	0.082028	1	0.140715	1	0.006724	4	0.042627	4	0.010017	3	0.090501	3	0.026713	2	0.099203	2
		λ	−0.01474	3	0.084148	1	−0.00541	4	0.075748	2	−0.01495	4	0.081042	3	0.024655	1	0.081247	2
		∑ Rank	6		3		12		10		10		9		4		6	
	100	α	0.016829	2	0.453821	1	−0.00126	4	0.085145	4	0.015741	3	0.301315	3	0.059674	1	0.389176	2
		θ	0.016211	1	0.124052	1	0.003828	4	0.036019	4	0.009168	3	0.084335	3	0.015022	2	0.091723	2
		λ	−0.01387	3	0.080529	1	−0.00248	4	0.065027	2	−0.0149	4	0.079522	2	0.008973	1	0.071036	3
		∑ Rank	6		3		12		10		10		8		4		7	
	200	α	0.014146	2	0.241456	1	−0.00114	4	0.031091	4	0.014128	3	0.166741	2	0.030725	1	0.128756	3
		θ	0.002011	3	0.066863	1	0.000717	4	0.02494	4	0.0082	1	0.051008	3	0.005046	2	0.052854	2
		λ	−0.0022	3	0.076778	1	−0.00137	4	0.047154	2	−0.00922	4	0.06048	3	0.008912	1	0.068712	2
		∑ Rank	8		3		12		10		8		8		4		7	
	Total rank		11			22			16			11						
0.5	25	α	0.337683	1	0.50644	1	0.090933	4	0.146	4	0.336589	2	0.45835	2	0.217261	3	0.258538	3
		θ	0.111395	1	0.297497	1	0.036013	4	0.166826	4	0.110824	2	0.265625	2	0.100963	3	0.179842	3
		λ	−0.05131	4	0.395424	1	−0.03217	4	0.143998	2	−0.05129	3	0.313146	2	−0.00881	1	0.20029	3
		∑ Rank	6		3		12		10		7		6		7		9	
	70	α	0.207274	1	0.26776	2	0.05815	4	0.109132	4	0.206881	2	0.301125	1	0.124303	3	0.1626	3
		θ	0.090973	1	0.194696	1	0.034912	4	0.095431	4	0.090931	2	0.192916	2	0.076127	3	0.118987	3
		λ	−0.045	3	0.284272	1	−0.01976	4	0.120023	2	−0.0452	4	0.220632	2	0.001959	1	0.150957	3
		∑ Rank	5		4		12		10		8		5		7		9	
	100	α	0.192792	2	0.247364	2	−0.01696	4	0.066954	4	0.193514	1	0.261325	1	0.100436	3	0.156027	3
		θ	0.089484	2	0.176863	1	−0.03058	4	0.090415	4	0.089562	1	0.176665	2	0.046063	3	0.109306	3
		λ	−0.04356	4	0.229272	1	0.018205	4	0.072571	1	−0.04056	3	0.202952	2	0.001209	2	0.134832	3
		∑ Rank	8		4		12		9		5		5		8		9	
	200	α	0.149399	1	0.185062	2	−0.00283	4	0.024367	4	0.148784	2	0.188903	1	0.043033	3	0.092727	3
		θ	0.080922	1	0.148105	1	−0.0102	4	0.030511	4	0.07918	2	0.13829	2	0.018522	3	0.077706	3
		λ	−0.03657	4	0.202376	1	−0.00198	4	0.030395	2	−0.03465	3	0.157082	2	0.001143	1	0.10759	3
		∑ Rank	6		4		12		10		7		5		7		9	
	Total rank		10			22			12			16						
∑ Total rank			21			44			28			27						

Since Eq. (24) cannot be solved explicitly, numerical methods are used. One of the most effective numerical approaches in Bayesian estimation is the Monte Carlo Markov chain method. In this case, we propose using the Metropolis–Hastings algorithm, see the study by Tierney [59].

7 Simulation

The simulation of four estimation methods deepens our understanding of statistical techniques, assists in choosing the most appropriate method, and reveals the strengths and weaknesses of various approaches in different contexts. This section utilizes simulation analysis to compare the results of three different parameter estimates for the SPB-X distribution. We carried out simulations by generating 10,000 RS with sizes of n = 25, 70, 100, and 200 from the SPB-X distribution, applying various parameter values $(\alpha, \theta, \lambda)$ = (0.5, 0.5, 0.75), (1.5, 0.5, 0.75), (0.5, 0.5, 2), (1.5, 0.5, 2), (1.5, 2, 2), (3, 1.5, 1.5), (3, 1.5, 3), and (1.5, 4, 2). We computed the root mean square error (RMSE) and relative absolute bias (RAB) for all estimates, which are essential metrics to evaluate the performance of different estimators. The simulations were performed using the R

Table 5: RAB, RMSE, and ranked of estimation methods for parameters of SPB-X distribution

$\theta = 0.5, \lambda = 2$			MLE				LS				MPS				Bayeaisan			
α	n		RAB		RMSE		RAB		RMSE		RAB		RMSE		RAB		RMSE	
0.5	25	α	0.237293	1	0.481939	1	0.031422	4	0.140239	4	0.236122	2	0.369424	2	0.148007	3	0.178753	3
		θ	0.094034	1	0.313662	1	−0.02126	3	0.159829	4	0.079784	2	0.249774	2	0.069063	3	0.122545	4
		λ	−0.08233	3	0.56169	1	−0.09085	4	0.191695	4	−0.08216	2	0.487931	2	−0.00937	1	0.246092	3
		∑ Rank	5		3		11		12		6		6		7		10	
	70	α	0.135257	2	0.290683	1	0.030646	4	0.086505	4	0.135534	1	0.230553	2	0.071858	3	0.10814	3
		θ	0.065682	2	0.188634	1	0.010859	3	0.083362	4	0.065696	1	0.154763	2	0.035749	3	0.081059	4
		λ	−0.05906	4	0.463898	1	−0.01577	4	0.166698	2	−0.05888	3	0.392399	2	−0.00845	1	0.215204	3
		∑ Rank	8		3		11		10		5		6		7		10	
	100	α	0.108458	1	0.191718	1	−0.02193	4	0.068469	4	0.108304	2	0.181584	2	0.059705	3	0.097331	3
		θ	0.059619	1	0.129028	1	−0.00774	4	0.068863	4	0.059537	2	0.126247	2	0.033491	3	0.078193	3
		λ	−0.05741	4	0.373276	1	0.004215	4	0.0915	1	−0.05714	3	0.345385	2	−0.0071	2	0.204391	3
		∑ Rank	6		3		12		9		7		6		8		9	
	200	α	0.080716	1	0.065794	2	0.002218	4	0.038939	4	0.080353	2	0.12508	1	0.043635	3	0.060712	3
		θ	0.053007	1	0.058535	2	−0.00176	4	0.038808	4	0.052625	2	0.096398	1	0.028389	3	0.050202	3
		λ	−0.04536	4	0.184168	2	0.00109	4	0.040365	1	−0.04513	3	0.292117	1	−0.0061	2	0.179928	3
		∑ Rank	6		6		12		9		7		3		8		9	
	Total rank		12			21			10			17						
1.5	25	α	−0.05385	4	0.533336	1	−0.02125	4	0.214276	2	−0.03524	3	0.434168	2	0.041754	1	0.420127	3
		θ	−0.08557	3	0.225968	1	−0.0937	3	0.200131	4	−0.08501	2	0.203626	2	0.005053	1	0.082185	4
		λ	−0.08693	4	0.416789	1	0.058698	3	0.228875	1	−0.07017	3	0.355903	2	0.002684	2	0.208831	4
		∑ Rank	11		3		10		7		8		6		4		11	
	70	α	0.036452	1	0.153281	2	−0.0086	4	0.115467	4	0.00494	3	0.385402	1	0.034544	2	0.131382	3
		θ	−0.02989	4	0.151305	2	−0.02655	3	0.12475	2	−0.02898	3	0.163303	1	0.004341	1	0.065997	4
		λ	−0.01584	2	0.143572	2	−0.01689	4	0.123425	4	−0.01638	3	0.292842	1	0.002335	1	0.129063	3
		∑ Rank	7		6		11		10		9		3		4		10	
	100	α	0.019642	2	0.125253	2	−0.00629	4	0.08095	4	0.00382	3	0.344566	1	0.031589	1	0.123064	3
		θ	−0.00937	3	0.137042	1	−0.01914	3	0.093568	4	−0.00932	2	0.136492	2	0.003622	1	0.060676	4
		λ	−0.01138	3	0.12584	2	0.001803	3	0.109926	1	−0.01141	4	0.271943	1	−0.00214	2	0.108031	4
		∑ Rank	8		5		10		9		9		4		4		11	
	200	α	0.017144	2	0.123611	2	−0.00254	4	0.070877	4	0.00276	3	0.300586	1	0.023573	1	0.092434	3
		θ	0.008163	2	0.105762	1	−0.01064	3	0.081686	4	0.008167	1	0.089414	2	0.001453	3	0.055692	4
		λ	−0.01047	3	0.112907	2	−0.00149	4	0.086068	2	−0.01068	4	0.222332	1	−0.0013	1	0.091578	3
		∑ Rank	7		5		11		10		8		4		5		10	
	Total rank		12			21			12			15						
∑ Total rank			24			42			22			32						

programming language, and the results, including the RAB and RMSE values, are summarized in Tables 4–7 for the MLE, least squares (LS), MPS, and Bayesian estimation methods. Simulating these four estimation techniques for the SPB-X distribution's parameters plays a crucial role in statistical research and analysis for several key reasons:

- Simulations allow researchers to assess the performance of various estimation methods under different conditions. By generating synthetic datasets with known properties, they can evaluate the accuracy, rank, RMSE, and RAB of each technique.
- Simulations serve as a tool to optimize estimation techniques for the parameters of the SPB-X distribution. Researchers can adjust the algorithm parameters or experiment with alternative methodologies to determine the most efficient and accurate approach for specific scenarios.
- Through simulation studies, researchers can systematically compare multiple estimators for the SPB-X distribution parameters within a controlled setting. This facilitates an objective assessment of each method's advantages and limitations, guiding the selection of the most suitable estimator for practical use.

Tables 4, 5, 6, and 7 contain RMSE and RAB values, which are standard metrics used to assess the precision and bias of the different estimation methods. Lower RMSE values

Table 6: RAB, RMSE, and ranked of estimation methods for parameters of SPB-X distribution

$\alpha = 1.5, \lambda = 2$			MLE				LS				MPS				Bayeaisan			
θ	n		RAB		RMSE		RAB		RMSE		RAB		RMSE		RAB		RMSE	
2	25	α	−0.0417	4	0.784902	1	−0.0408	4	0.186499	3	−0.0312	2	0.618933	2	0.0798	1	0.452759	3
		θ	−0.0379	4	0.36032	1	−0.0102	2	0.286095	2	−0.0377	3	0.274264	3	0.0082	1	0.191702	4
		λ	0.038	2	0.756547	1	−0.0094	4	0.203331	4	0.0385	1	0.599379	2	−0.0039	3	0.249373	3
		∑ Rank	10		3		10		9		6		7		5		10	
	70	α	−0.0159	4	0.675556	1	0.006	4	0.178961	2	−0.0156	3	0.402374	2	0.052	1	0.323463	3
		θ	−0.0258	3	0.203099	1	−0.0056	2	0.19451	2	−0.026	4	0.163596	3	0.0068	1	0.110154	4
		λ	0.0093	1	0.711175	1	−0.0084	4	0.169255	4	0.0088	2	0.353533	2	0.0037	3	0.213583	3
		∑ Rank	8		3		10		8		9		7		5		10	
	100	α	0.0069	2	0.466559	1	−0.0054	4	0.13176	4	0.0069	2	0.361317	2	0.044	1	0.295145	3
		θ	−0.0165	4	0.172465	1	0.0039	2	0.168627	2	−0.0163	3	0.135038	3	0.0055	1	0.084145	4
		λ	0.0084	1	0.553203	1	0.002	4	0.142907	4	0.0075	2	0.314431	2	0.0035	3	0.204128	3
		∑ Rank	7		3		10		10		7		7		5		10	
	200	α	−0.006	3	0.452244	1	0.0043	4	0.128513	2	−0.006	3	0.26335	3	0.0434	1	0.26658	2
		θ	−0.0094	3	0.109653	1	−0.0027	2	0.107198	2	−0.0095	4	0.093364	3	0.0055	1	0.058806	4
		λ	0.0025	1	0.499037	1	−0.0015	4	0.134906	4	0.0021	3	0.237421	2	0.0025	1	0.191229	3
		∑ Rank	7		3		10		8		10		8		3		9	
	Total rank		10			18			18			12						
4	25	α	0.0987	1	0.807114	1	−0.0536	3	0.480387	4	0.0206	3	0.603981	2	0.056	2	0.442574	4
		θ	−0.0464	3	0.90611	1	−0.0071	4	0.443569	1	−0.0467	4	0.68943	2	−0.0088	2	0.46061	3
		λ	0.0096	2	0.416854	1	0.0241	4	0.1636	1	0.0057	3	0.402546	2	0.0028	4	0.210831	3
		∑ Rank	6		3		11		6		10		6		8		10	
	70	α	0.015	2	0.405756	2	−0.027	4	0.253711	4	0.0145	3	0.429374	1	0.0523	1	0.359802	3
		θ	−0.029	4	0.725479	1	−0.0065	4	0.243816	2	−0.0284	3	0.462748	2	−0.0019	1	0.380727	3
		λ	−0.0079	4	0.396709	1	0.0134	4	0.123397	1	−0.0048	3	0.284519	2	−0.0009	2	0.185777	3
		∑ Rank	10		4		12		7		9		5		4		9	
	100	α	0.014	2	0.327157	2	−0.007	4	0.212561	4	0.0136	3	0.382202	1	0.0466	1	0.314589	3
		θ	−0.0229	4	0.306385	2	−0.0022	4	0.18737	2	−0.0227	3	0.385213	1	0.0014	1	0.306162	3
		λ	−0.0074	4	0.155957	2	0.0061	4	0.058291	1	−0.0037	3	0.227913	1	−0.0008	2	0.149529	3
		∑ Rank	10		6		12		7		9		3		4		9	
	200	α	0.0141	2	0.323692	1	−0.0062	4	0.187806	4	0.0124	3	0.28776	2	0.0426	1	0.266214	3
		θ	−0.0205	4	0.290651	2	−0.0012	4	0.175217	1	−0.0125	3	0.302992	1	−0.0013	2	0.229806	3
		λ	−0.0013	3	0.13804	2	0.0051	4	0.046913	1	−0.0037	4	0.189102	1	−0.0003	2	0.126885	3
		∑ Rank	9		5		12		6		10		4		5		9	
	Total rank		14			18			14			14						
∑ Total rank			24			36			32			26						

suggest more accurate estimates, while lower RAB values suggest less bias. You can see in the tables how the performance of each method changes as the sample size increases. Typically, as sample sizes increase (n = 200), the RMSE and RAB values are expected to decrease, reflecting improved estimation performance. The ranking system (1st, 2nd, 3rd, 4rd) shows which method is best suited for a particular condition. For example, a method ranked "1st" consistently across different parameter settings and sample sizes would indicate it is the most reliable estimator in that situation. The total rank column provides an overall assessment of each method across all conditions. This helps summarize which estimation method is generally superior in terms of various sample sizes and parameter values. A method with consistently low total ranks (closer to 1) is likely the most robust estimator overall.

The best-performing estimation method can be determined using the total rank column in the table. The method with the highest total rank is considered the most effective in different scenarios. Based on the ranked values provided in the table, it is clear which method consistently achieves better performance in terms of RMSE and RAB. In the case of $\theta = 0.5, \lambda = 0.75$, we observe that the LS method performs the best, achieving a total rank of 201. This is the highest value compared to the other estimation methods, indicating its superior performance in this

Table 7: RAB, RMSE, and ranked of estimation methods for parameters of SPB-X distribution

$\alpha = 3, \theta = 1.5$			MLE				LS				MPS				Bayeaisan			
λ	n		RAB		RMSE		RAB		RMSE		RAB		RMSE		RAB		RMSE	
1.5	25	α	−0.08714	4	−0.00711	1	−0.08685	3	−0.0297	2	1.022988	1	0.247263	4	0.749682	2	0.65512	3
		θ	−0.0439	3	−0.0164	2	−0.0439	4	−0.00941	1	0.171082	2	0.263046	1	0.142879	3	0.124047	4
		λ	0.03102	1	−0.0128	4	0.030965	2	0.011691	3	0.721195	1	0.274253	3	0.431103	2	0.210736	4
		∑ Rank	8		7		9		6		4		8		7		11	
	70	α	−0.06098	4	−0.00626	2	−0.06064	3	0.021909	1	0.203063	3	0.164013	4	0.601484	2	0.617428	1
		θ	−0.03047	4	−0.0035	1	−0.03033	3	−0.00523	2	0.063614	4	0.070686	3	0.099399	1	0.085748	2
		λ	0.021379	1	−0.00875	4	0.0211	2	0.005284	3	0.148033	4	0.165576	3	0.292466	1	0.175084	2
		∑ Rank	9		7		8		6		11		10		4		5	
	100	α	−0.04945	4	−0.00506	2	−0.0494	3	0.005074	1	0.20064	3	0.153381	4	0.500061	2	0.567637	1
		θ	−0.02241	3	−0.00337	1	−0.02243	4	−0.00504	2	0.061136	3	0.06013	4	0.078926	1	0.078552	2
		λ	0.018067	1	0.001437	4	0.01782	2	0.004198	3	0.127727	4	0.139024	3	0.226073	1	0.167588	2
		∑ Rank	8		7		9		6		10		11		4		5	
	200	α	−0.02843	4	−0.00214	1	−0.02818	3	−0.00465	2	0.186027	3	0.148856	4	0.36416	2	0.522604	1
		θ	−0.01255	4	−0.00153	1	−0.01253	3	−0.0036	2	0.060114	2	0.043521	4	0.055014	3	0.062995	1
		λ	0.005953	1	−0.00078	4	0.005789	2	0.004023	3	0.052092	4	0.100627	3	0.147558	2	0.153146	1
		∑ Rank	9		6		8		7		9		11		7		3	
1.5	Total rank		15			15			20			10						
3	25	α	−0.05279	3	−0.00454	1	−0.05289	4	−0.01405	2	1.01585	1	0.304876	4	0.685717	2	0.670245	3
		θ	−0.03089	3	−0.02071	2	−0.03092	4	−0.00838	1	0.281515	2	0.322409	1	0.134832	3	0.123108	4
		λ	−0.00966	3	−0.01596	4	−0.00953	2	0.00603	1	0.954966	1	0.464819	3	0.569249	2	0.250907	4
		∑ Rank	9		7		10		4		4		8		7		11	
	70	α	−0.03685	4	−0.00304	2	−0.03662	3	0.011103	1	0.206847	3	0.111765	4	0.553092	1	0.545158	2
		θ	−0.01952	4	−0.00439	2	−0.0195	3	−0.00201	1	0.194985	1	0.152068	2	0.093001	3	0.088362	4
		λ	0.002145	2	−0.00756	4	0.001838	3	0.002758	1	0.247989	2	0.22598	3	0.397819	1	0.219657	4
		∑ Rank	10		8		9		3		6		9		5		10	
	100	α	−0.02922	3	−0.00237	2	−0.02956	4	0.010222	1	0.189243	3	0.102759	4	0.481484	2	0.511498	1
		θ	−0.01546	4	−0.00407	2	−0.01544	3	0.001072	1	0.156499	1	0.148069	2	0.078632	3	0.075901	4
		λ	0.001646	3	−0.00279	4	0.001779	1	0.001779	2	0.142582	4	0.216851	3	0.344835	1	0.220094	2
		∑ Rank	10		8		8		4		8		9		6		7	
	200	α	−0.02282	3	−0.00218	2	−0.02284	4	0.009103	1	0.146666	3	0.091199	4	0.367609	2	0.413775	1
		θ	−0.01258	3	−0.00172	2	−0.01261	4	−0.00091	1	0.152245	1	0.043352	4	0.054523	3	0.055331	2
		λ	0.000397	3	0.000944	2	0.000335	4	0.001427	1	0.137847	4	0.159341	3	0.251225	1	0.186038	2
		∑ Rank	9		6		12		3		8		11		6		5	
	Total rank		15			15			19			11						
∑ Total rank			30			30			39			21						

scenario. In the case of $\theta = 0.5, \lambda = 2$, we observe that the Bayesian estimation method performs the best, achieving a total rank of 221. This is the highest value compared to the other estimation methods, indicating its superior performance in this scenario. In the case of $\alpha = 1.5, \lambda = 2$, we observe that the LS method performs the best, achieving a total rank of 173. This is the highest value compared to the other estimation methods, indicating its superior performance in this scenario.

In all cases, the LS method achieved the highest total rank, reaching 546, indicating its superior performance. The Bayesian method followed with a total rank of 494. However, the MLE method had the lowest performance, with a total rank of 327, making it the least effective among the estimation methods compared.

7.1 Approximate confidence intervals (ACIs)

Determining the exact distribution of these estimates becomes problematic when closed-form MLEs and MPS for the unknown parameters cannot be obtained. Therefore, it is not feasible to obtain precise confidence intervals (CIs) for the parameters. Hence, ACIs are built using large sample approximation approaches for the parameters α, θ, and λ to overcome this constraint.

Using the asymptotic normality features of MLEs and MPS, one may compute the ACIs for $\Theta = (\alpha, \theta, \lambda)$, which are generated from the observed Fisher information matrix. For the purpose of approximating the asymptotic variance–covariance of the MLEs and MPS, the observed information matrix is obtained by differentiating the log-likelihood function with respect to the unknown parameters.

$$I(\hat{\Theta}) = \left(\frac{\partial^2 L}{\partial \Theta_i \partial \Theta_j}\right)_{\langle \hat{\Theta} \rangle}. \tag{25}$$

From there, we can obtain the approximate asymptotic variance–covariance matrix, which is:

$$\mathrm{Cov}(\hat{\vartheta}) = I^{-1}(\hat{\vartheta}). \tag{26}$$

With a mean of Θ and a variance–covariance matrix of $\mathrm{Cov}(\hat{\Theta})$, $\hat{\Theta} \sim N(\Theta, \mathrm{Cov}(\hat{\Theta}))$, the MLEs and MPS parameters are

Table 8: Confidence intervals for parameters of SPB-X distribution

			$\theta = 0.5, \lambda = 0.75$							$\theta = 2, \lambda = 0.75$					
			MLE			MPS				MLE			MPS		
α	n		Lower	Upper	LACI	Lower	Upper	LACI	α	Lower	Upper	LACI	Lower	Upper	LACI
1.5	25	α	0.6388	2.6563	2.0175	0.5157	2.5684	2.0527	0.5	0.0699	1.1674	1.0975	0.0416	1.3042	1.3722
		θ	0.2435	0.8438	0.6003	0.2617	0.8244	0.5627		0.1030	0.9910	0.8880	0.0566	1.0232	0.9665
		λ	0.3444	1.1780	0.8337	0.3998	1.1281	0.7282		0.7828	2.8879	2.1051	0.9352	2.7361	1.8010
	70	α	0.6004	2.5934	1.9930	0.8893	2.1600	1.2707		0.0135	1.1217	1.1082	0.1358	0.9997	0.8638
		θ	0.2772	0.8048	0.5277	0.3279	0.6821	0.3542		0.1688	0.8969	0.7282	0.2364	0.8293	0.5928
		λ	0.5754	0.9024	0.3270	0.5815	0.8961	0.3146		1.0026	2.7611	1.7585	1.1486	2.6159	1.4673
	100	α	0.6371	2.4134	1.7762	0.9349	2.1124	1.1775		0.1938	0.9147	0.7208	0.2144	0.8939	0.6794
		θ	0.2655	0.7507	0.4852	0.3395	0.6696	0.3301		0.2838	0.7759	0.4921	0.2893	0.7702	0.4809
		λ	0.5831	0.8961	0.3130	0.5845	0.8931	0.3086		1.1890	2.5813	1.3923	1.2469	2.5245	1.2776
	200	α	1.0498	1.9926	0.9428	1.1970	1.8454	0.6483		0.4385	0.6422	0.2037	0.3080	0.7723	0.4643
		θ	0.3700	0.6320	0.2621	0.4044	0.6038	0.1993		0.4242	0.6288	0.2046	0.3445	0.7081	0.3635
		λ	0.5979	0.8988	0.3009	0.6253	0.8609	0.2355		1.5951	2.2234	0.6283	1.3652	2.4543	1.0891
0.5	25	α	0.0665	1.2712	1.2047	1.1693	2.8405	1.6712	1.5	0.3859	2.4525	2.0666	0.4039	2.4903	2.0864
		θ	0.1593	0.9520	0.7927	0.0462	1.0646	1.0183		0.0223	0.8921	0.8698	0.0672	0.8478	0.7806
		λ	0.1095	1.3135	1.2040	0.1024	1.3207	1.2182		1.0837	2.5686	1.4849	1.2186	2.5007	1.2821
	70	α	0.1197	1.0875	0.9678	0.0492	1.1577	1.1086		1.2740	1.8353	0.5613	0.5488	2.4660	1.9172
		θ	0.1744	0.9165	0.7421	0.1780	0.9129	0.7349		0.1899	0.7802	0.5902	0.1667	0.8043	0.6376
		λ	0.1630	1.2695	1.1065	0.2888	1.1434	0.8546		1.6939	2.2428	0.5489	1.3969	2.5376	1.1407
	100	α	0.1499	1.0429	0.8930	0.1210	1.0726	0.9516		1.2909	1.7681	0.4772	0.6243	2.3871	1.7628
		θ	0.2094	0.8801	0.6708	0.2098	0.8797	0.6699		0.2269	0.7638	0.5369	0.2280	0.7627	0.5347
		λ	0.2725	1.1621	0.8896	0.3263	1.1129	0.7866		1.7347	2.2198	0.4852	1.4460	2.5083	1.0623
	200	α	0.2428	0.9066	0.6637	0.2341	0.9147	0.6807		1.2887	1.7627	0.4740	0.7085	2.2998	1.5913
		θ	0.2612	0.8197	0.5585	0.2799	0.7993	0.5194		0.2969	0.7112	0.4143	0.3290	0.6792	0.3501
		λ	0.3296	1.1156	0.7860	0.4204	1.0277	0.6073		1.7616	2.1965	0.4349	1.4875	2.4698	0.9823

Table 9: Confidence intervals for parameters of SPB-X distribution: $\alpha = 1.5, \lambda = 2$

$\alpha = 1.5, \lambda = 2$			MLE			MPS		
θ	n		Lower	Upper	LACI	Lower	Upper	LACI
2	25	α	0.1006	2.7742	2.6736	0.2748	2.6940	2.4193
		θ	1.2337	2.6145	1.3808	1.4078	2.4416	1.0338
		λ	0.6007	3.5513	2.9507	0.9118	3.2420	2.3301
	70	α	0.1529	2.7994	2.6465	0.7049	2.2795	1.5746
		θ	1.5634	2.3334	0.7700	1.6439	2.2519	0.6079
		λ	0.6251	3.4119	2.7869	1.3256	2.7097	1.3841
	100	α	0.5962	2.4246	1.8285	0.7955	2.2113	1.4158
		θ	1.6352	2.2989	0.6636	1.7105	2.2241	0.5136
		λ	0.9330	3.1006	2.1676	1.3994	2.6305	1.2312
	200	α	0.6048	2.3772	1.7724	0.9811	2.0129	1.0317
		θ	1.7694	2.1929	0.4235	1.8019	2.1603	0.3584
		λ	1.0269	2.9830	1.9561	1.5389	2.4695	0.9305
4	25	α	0.0929	3.2031	3.1102	0.3280	2.6925	2.3645
		θ	2.0762	5.5530	3.4768	2.5125	5.1142	2.6016
		λ	1.2031	2.8354	1.6323	1.2227	2.8000	1.5774
	70	α	0.7285	2.3166	1.5881	0.6667	2.3477	1.6810
		θ	2.4804	5.2877	2.8073	3.0071	4.7654	1.7583
		λ	1.2073	2.7611	1.5539	1.4331	2.5478	1.1147
	100	α	0.8811	2.1609	1.2798	0.7588	2.2549	1.4961
		θ	3.3354	4.4815	1.1461	3.1756	4.6432	1.4677
		λ	1.6810	2.2896	0.6086	1.5461	2.4390	0.8929
	200	α	0.8880	2.1542	1.2662	0.9434	2.0690	1.1257
		θ	3.3715	4.4646	1.0931	3.3643	4.5357	1.1715
		λ	1.7269	2.2679	0.5410	1.6222	2.3629	0.7407

Table 10: MLE for parameters of SPB-X and each competitive models: latitude for the Southwest of the rain gauge stations

		Estimates	StEr	KSD	PVKS	CVM	PVCVM	AD	PVAD
SPB-X	α	14.5195	91.8156	0.1684	0.9141	0.0380	0.9417	0.3073	0.9254
	θ	0.8207	2.1497						
	λ	1.0578	2.2285						
PB-X	α	5.2896	19.5810	0.1709	0.9049	0.0385	0.9391	0.3103	0.9207
	θ	0.4440	1.1365						
	λ	1.8414	2.6215						
SEWHE	α	2.5621	7.9144	0.1740	0.8932	0.0506	0.9341	0.3817	0.9218
	θ	3.1999	5.2423						
	λ	1.4554	4.0546						
	β	0.3341	0.1767						
W	α	8.0720	1.9099	0.1764	0.8834	0.0579	0.8369	0.4090	0.8368
	θ	2.0251	0.0800						
G	α	51.0781	18.4243	0.1703	0.9042	0.03914	0.9352	0.3116	0.9179
	θ	0.0374	0.0135						
EW	α	0.6437	0.4917	0.1709	0.9050	0.0404	0.9391	0.3204	0.9207
	θ	3.6794	5.2306						
	λ	5.3017	19.6086						

Table 11: MLE for parameters of SPB-X and each competitive models: latitude for West of rain gauge stations

		Estimates	StEr	KSD	PVKS	CVM	PVCVM	AD	PVAD
SPB-X	α	2.7126	9.3506	0.1036	0.9978	0.0196	0.9960	0.1702	0.9949
	θ	0.2305	0.9371						
	λ	1.0543	1.9056						
PB-X	α	1.8090	4.3094	0.1038	0.9976	0.0197	0.9952	0.1703	0.9940
	θ	0.1305	0.4589						
	λ	1.4638	1.7972						
SEWHE	α	0.7708	2.8499	0.1417	0.9422	0.0329	0.9927	0.2473	0.9913
	θ	3.1580	9.7527						
	λ	0.1476	0.6489						
	β	0.1821	0.2501						
W	α	4.0489	0.9208	0.1201	0.9866	0.02484	0.9926	0.1920	0.9928
	θ	4.6803	0.3525						
G	α	12.5199	5.0407	0.1129	0.9932	0.0220	0.9954	0.1884	0.9936
	θ	0.3383	0.1390						
EW	α	0.2487	0.1808	0.1038	0.9968	0.0223	0.9962	0.1817	0.9920
	θ	2.9275	3.7318						
	λ	1.8087	4.4687						

roughly distributed according to a multivariate normal distribution. The ACIs for the unknown parameters can be expressed as $100(1-\varepsilon)\%$ for any $0<\varepsilon<1$.

$$\left(\hat{\Theta}-\rho_{\frac{\varepsilon}{2}}\sqrt{\mathrm{V\,ar}(\hat{\Theta})},\,\hat{\Theta}+\rho_{\frac{\varepsilon}{2}}\sqrt{\mathrm{V\,ar}(\hat{\Theta})}\right). \tag{27}$$

The $(1-\varepsilon)$ quantile of the standard normal distribution $N(0,1)$ is represented by $\rho_{\frac{\varepsilon}{2}}$.

Tables 8 and 9 present confidence intervals for the parameters (α,θ,λ) of the SPB-X distribution using the MLE and MPS methods for different sample sizes and parameter values. It shows that as the sample size increases,

Table 12: MLE for parameters of SPB-X and each competitive models: dataset of carbon fibers stress

		Estimates	StEr	KSD	PVKS	CVM	PVCVM	AD	PVAD
SPB-X	α	0.8472	0.4571	0.0784	0.8124	0.0809	0.8604	0.4809	0.8972
	θ	0.0878	0.0994						
	λ	1.8287	0.6911						
PB-X	α	0.8006	0.3533	0.0809	0.7801	0.0858	0.6861	0.5084	0.7619
	θ	0.1009	0.0829						
	λ	1.9554	0.5340						
SEWHE	α	4.6250	2.6478	0.0862	0.7112	0.0868	0.8398	0.4921	0.8694
	θ	0.4987	0.1811						
	λ	0.4402	0.2756						
	β	0.9296	0.2869						
SEWE	α	0.9319	0.2743	0.0812	0.7771	0.0821	0.7176	0.4811	0.7918
	θ	3.3898	0.5825						
	λ	0.0121	0.0107						
BIII	α	2.2416	0.1688	0.1941	0.0138	0.7133	0.0076	3.9874	0.0050
	θ	5.8443	0.8339						
W	α	3.4412	0.3309	0.0822	0.7630	0.0836	0.6727	0.4857	0.7607
	θ	3.0623	0.1149						
G	α	7.4880	1.2757	0.1328	0.1947	0.2461	0.1935	1.3107	0.2288
	θ	0.3685	0.0649						
EW	α	0.3094	0.0331	0.0809	0.7795	0.0813	0.6859	0.4847	0.7618
	θ	3.9118	1.0682						
	λ	0.8000	0.3528						

Table 13: MLE for parameters of SPB-X and each competitive models: dataset of carbon fibers strength

		Estimates	StEr	KSD	PVKS	CVM	PVCVM	AD	PVAD
SPB-X	α	0.8548	0.5113	0.0470	0.9980	0.0238	0.9995	0.2087	0.9981
	θ	0.2995	0.2240						
	λ	1.7155	0.7232						
PB-X	α	0.8131	0.3847	0.0479	0.9974	0.0259	0.9932	0.2236	0.9870
	θ	0.3759	0.1884						
	λ	1.8324	0.5392						
SEWHE	α	1.6525	2.5956	0.0477	0.9978	0.0239	0.9990	0.2093	0.9978
	θ	1.5192	2.5144						
	λ	0.5202	1.5503						
	β	0.5532	1.1950						
SEWE	α	0.8961	0.4053	0.0478	0.9978	0.0240	0.9959	0.2098	0.9912
	θ	3.2901	0.9324						
	λ	0.1064	0.0914						
BIII	α	3.2367	0.2923	0.1407	0.1304	0.3344	0.0782	2.1634	0.0588
	θ	2.0133	0.2424						
W	α	3.2489	0.3065	0.1201	0.9866	0.02484	0.9926	0.2920	0.9928
	θ	1.6171	0.0629						
G	α	6.9960	1.1629	0.0884	0.6535	0.1235	0.4824	0.8539	0.4432
	θ	0.2074	0.0357						
EW	α	0.5862	0.0712	0.0479	0.9973	0.0232	0.9932	0.2112	0.9870
	θ	3.6666	1.0799						
	λ	0.8124	0.3846						

the confidence intervals become narrower, indicating better precision. The lower limits, upper limits, and the length average of confidence intervals (LACIs) are computed. The MPS method generally produces slightly narrower intervals than MLE, suggesting better accuracy in some cases. Furthermore, confidence intervals vary according to parameter values, with broader intervals observed for $\theta = 0.5$ compared to $\theta = 2$. In general, the table highlights the comparative performance of the two estimation methods and the impact of sample size on the reliability of the estimation.

Table 15: MLE for parameters of SPB-X and each competitive models: insurance dataset

		Estimates	StEr	KSD	PVKS	CVM	PVCVM	AD	PVAD
SPB-X	α	16.8042	0.9714	0.0881	0.9463	0.0505	0.8767	0.3508	0.8949
	θ	0.2799	0.2559						
	λ	1.0771	47.5307						
PBX	α	0.7679	0.5972	0.0910	0.9319	0.0518	0.8687	0.3551	0.8910
	θ	0.4524	0.2740						
	λ	7.1741	12.1309						
SEWE	α	0.8713	0.5111	0.0915	0.9291	0.0525	0.8642	0.3583	0.8880
	θ	0.3280	0.4747						
	λ	6.7275	10.9735						
BIII	α	15.3663	4.8010	0.1442	0.4749	0.1413	0.4190	0.8172	0.4677
	θ	2.1054	0.2600						
W	α	2.0483	0.2612	0.0940	0.8939	0.0534	0.8657	0.3771	0.8701
	θ	5.9411	0.5431						
G	α	4.0985	0.9865	0.0988	0.8954	0.0532	0.8666	0.3898	0.8452
	θ	1.2798	0.3277						
EW	α	0.5570	0.7609	0.0909	0.9319	0.0517	0.8688	0.3549	0.8911
	θ	0.9054	0.5482						
	λ	7.1603	12.0956						

Table 14: Sed Excess of assets over liabilities for investment by insurance companies, and pension funds

Period	Value	Period	Value	Period	Value
1986	2.151	1997	4.301	2008	15.264
1987	2.208	1998	8.421	2009	4.547
1988	2.170	1999	6.661	2010	3.261
1989	2.707	2000	6.548	2011	3.426
1990	2.014	2001	4.977	2012	6.418
1991	1.698	2002	4.202	2013	7.389
1992	2.512	2003	5.580	2014	6.136
1993	4.857	2004	8.856	2015	5.820
1994	3.509	2005	6.902	2016	3.094
1995	5.066	2006	5.442	2017	8.216
1996	5.413	2007	8.067		

8 Applications

In this section, we present a comprehensive discussion of various statistical metrics used to evaluate the performance of different models [57]. Tables 10–15 provide a detailed comparison of key metrics, including estimates, standard errors (StEr), Kolmogorov-Smirnov distance (KSD), p-value for the Kolmogorov-Smirnov test (PVKS), Cramer-von Mises statistic (CVM), p-value for CVM (PVCVM), Anderson–Darling (AD) statistic, and p-value for AD (PVAD).

The performance of each model is presented in a detailed perspective, focusing on various distribution models, such as the power Burr X (PB-X) proposed by [22], the SEWHE by [42], Weibull (W) [52], gamma (G) [53], exponentiated Weibull (EW) [54], SEWE [42], and BIII [55] distributions.

8.1 Rainfall data analysis across Peninsular Malaysia

This study analyzed daily rainfall data collected from 50 rain gauge stations in Peninsular Malaysia during the period 1975–2004. Data were sourced from the Malaysian Meteorological Department and the Drainage and Irrigation Department. Following the regional classification by Dale (1959), the area was divided into five distinct rainfall zones: northwest, west, the Port Dickson–Muar

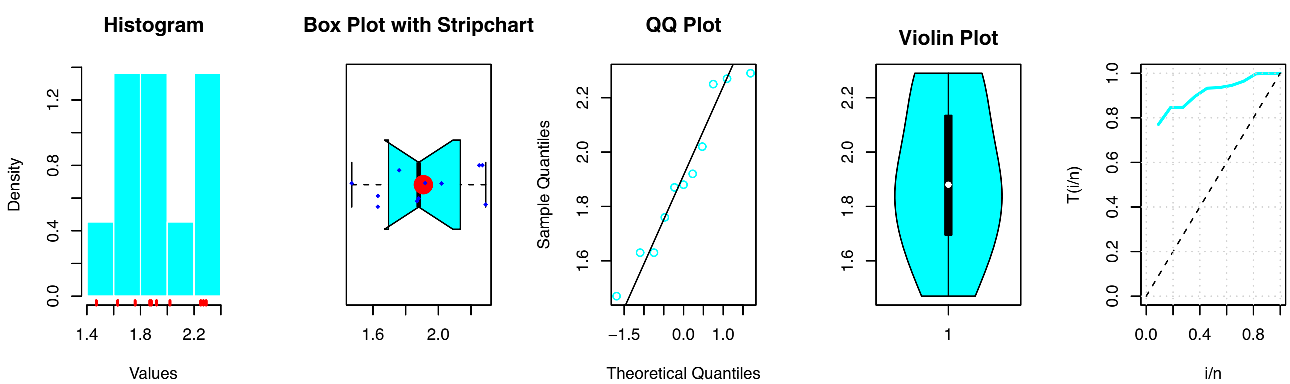

Figure 4: Some basic nonparametric plots for latitude for southwest of rain gauge stations.

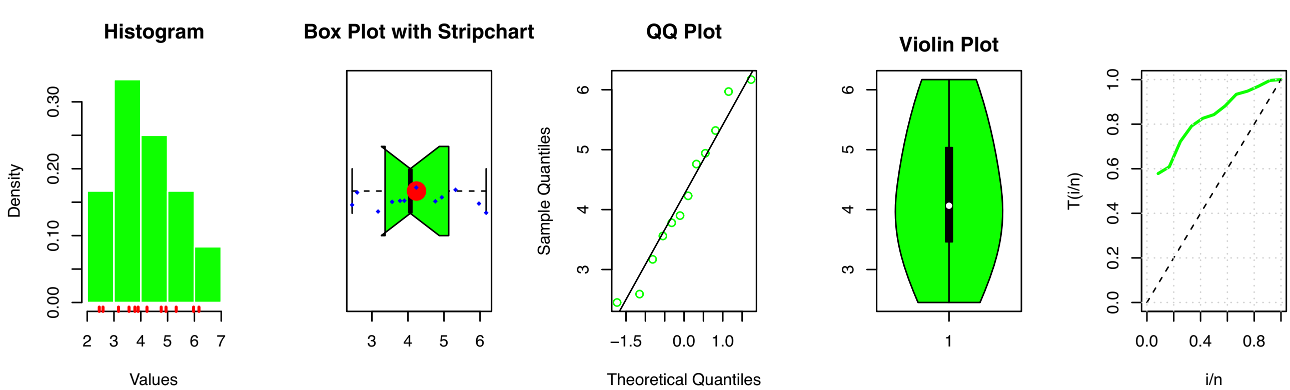

Figure 5: Some basic nonparametric plots for latitude for west of rain gauge stations.

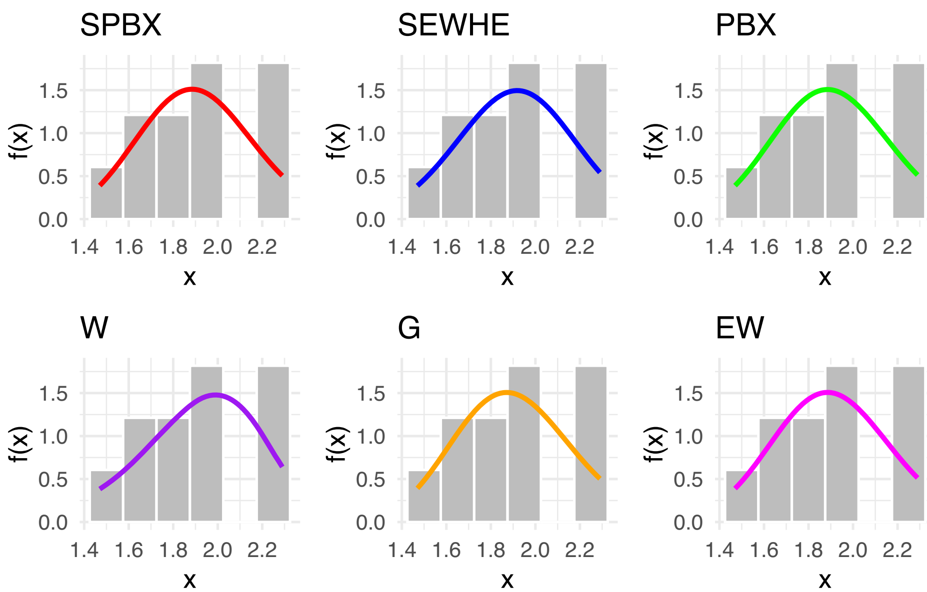

Figure 6: Estimated PDFs for the competing models for latitude for southwest of rain gauge stations.

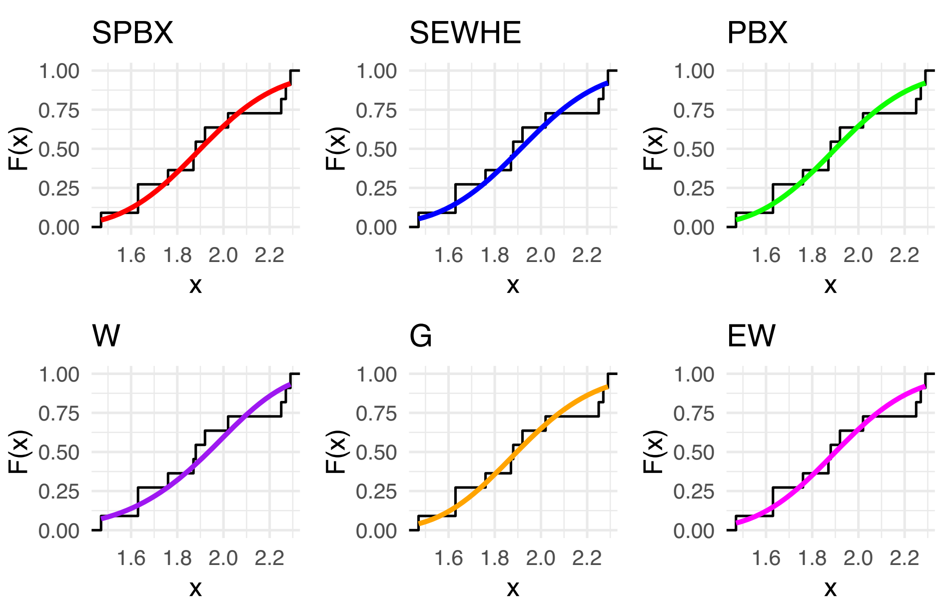

Figure 7: Estimated CDFs for the competing models for latitude for southwest of rain gauge stations.

coast, southwest, and east (Lim and Azizan [56]). Due to limited data availability, the ports on the port Dickson–Muar coast were grouped with the southwest region.

To ensure data reliability, the dataset was meticulously examined for missing values and homogeneity. Interestingly, less than 10% of the data was missing. The missing values were estimated using enhanced spatial weighting techniques [60], while homogeneity was verified through four robust statistical tests [61]: the standard normal homogeneity test, the Buishand range test, the Pettitt test, and the Von Neumann ratio test, as documented in [62].

Our analysis focused on the latitude data from two key regions, the Southwest and East. The latitude values for the Southwest region are: 1.47, 1.63, 1.63, 1.76, 1.87, 1.88, 1.92, 2.02, 2.25, 2.27, 2.29, and for the east region: 2.45, 2.59, 3.17, 3.56, 3.78, 3.90, 4.23, 4.76, 4.94, 5.32, 5.97, 6.17. In Tables 10 and 11, we provide an in-depth comparison of various models using MLE with StEr, KSD, PVKS, CVM, PVCVM,

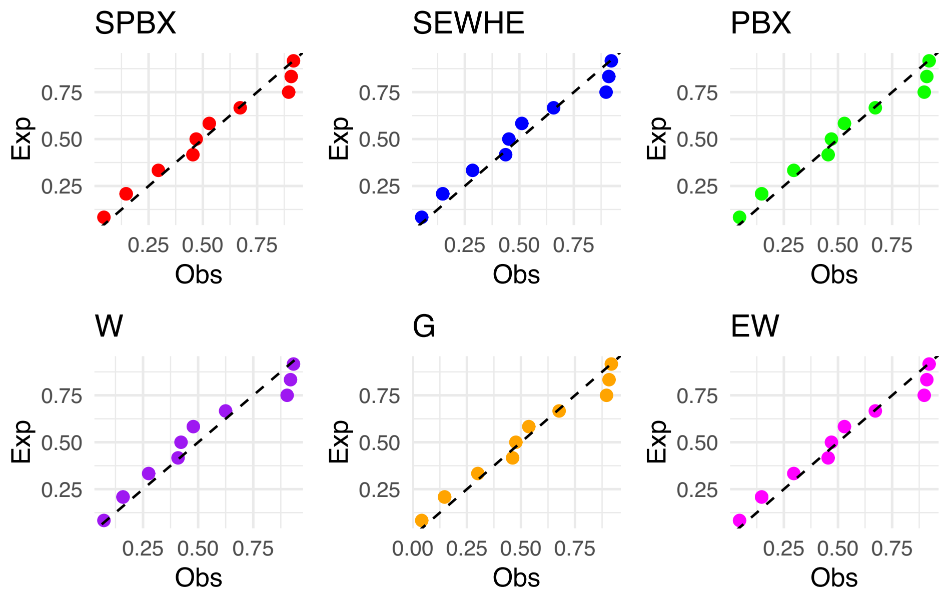

Figure 8: The PP plot for the competing models for latitude for southwest of rain gauge stations.

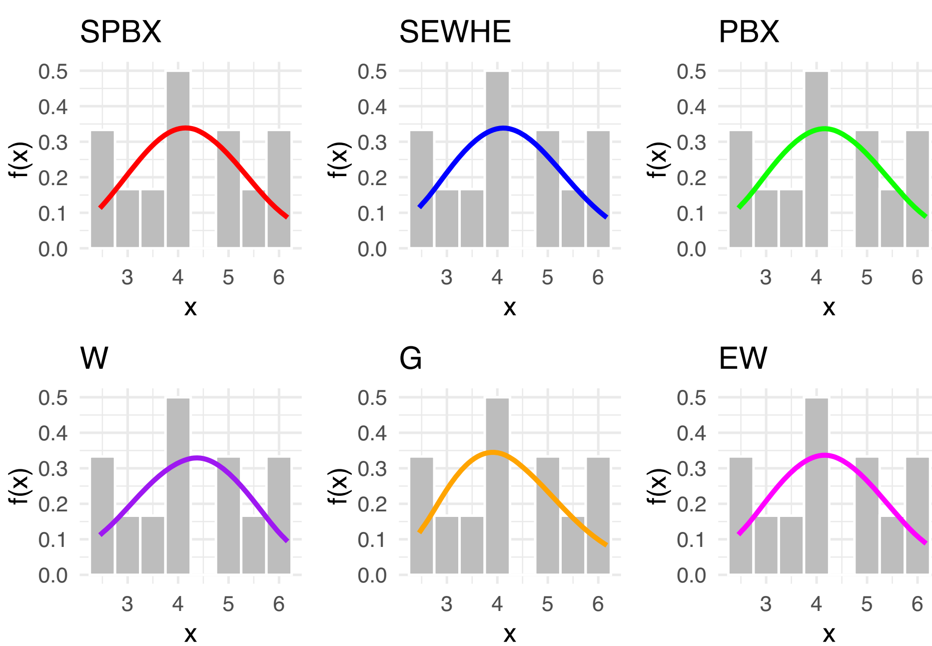

Figure 9: Estimated PDFs for the competing models for latitude for west of rain gauge stations.

AD, and PVAD. Among the tested distributions, the SPB-X distribution consistently outperformed others across multiple metrics, including KSD, PVKS, CVM, PVCVM, AD, and PVAD, making it the most suitable model for this rainfall dataset.

Figures 4 and 5 includes the histogram, violin plot, QQ (quantile-quantile) plot, box plot with stripchart, and TTT (total time in test) plot of dataset of rain gauge stations datasets. The estimated PDFs of competing models for the datasets of rain gauge stations datasets are shown in Figures 6 and 9, while Figures 7 and 10 display the estimated CDFs of the competitive models. Furthermore, Figures 8 and 11 illustrate the PP plots of the competing models. Figures 6–11 demonstrate the fit of our distribution to the actual data.

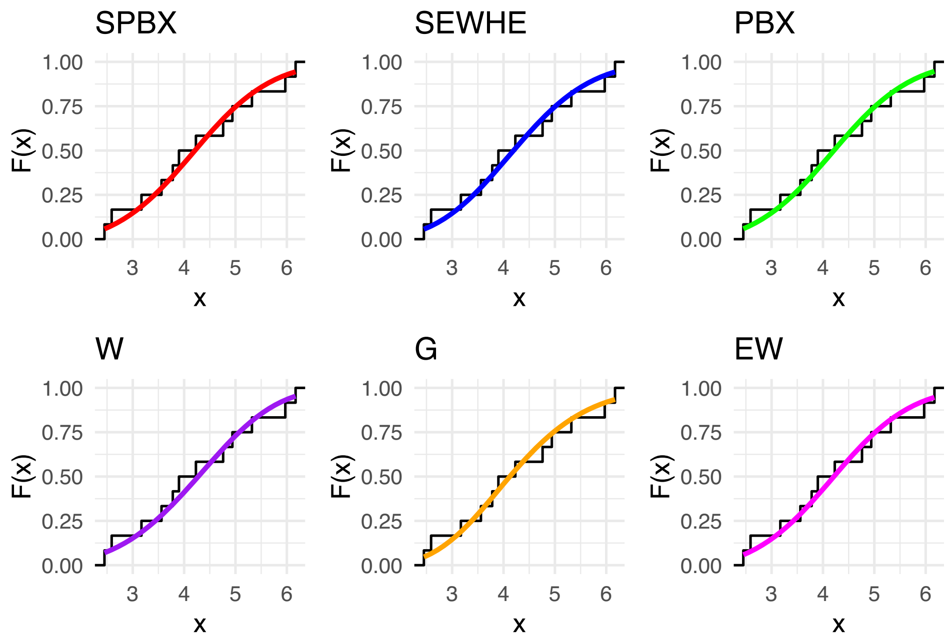

Figure 10: Estimated CDFs for the competing models for latitude for west of rain gauge stations.

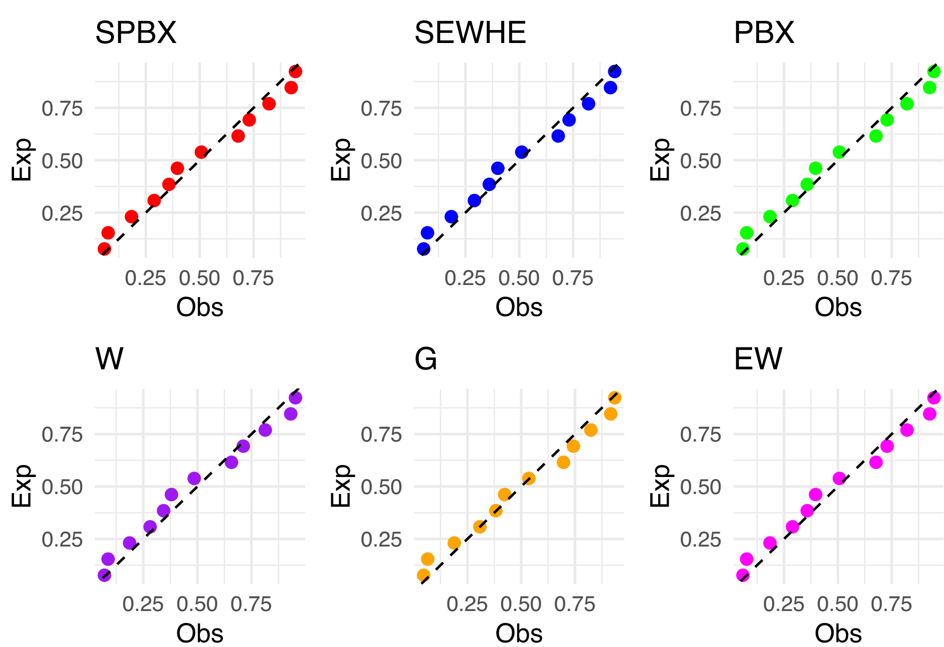

Figure 11: The PP plot for the competing models for latitude for west of rain gauge stations.

8.2 Breaking stress of carbon fibers dataset

The breaking stress of carbon fibers dataset contains crucial measurements of the maximum stress that carbon fibers can endure before fracturing. This dataset is indispensable for researchers and engineers in the fields of materials science and engineering. It plays a key role in investigating the mechanical properties and performance of carbon fiber-reinforced composites, widely used in industries such as aerospace and automotive manufacturing.

As mentioned by Cordeiro and Lemonte [40], this specific dataset offers valuable insights into the behavior of carbon fibers under stress. Below is the dataset:

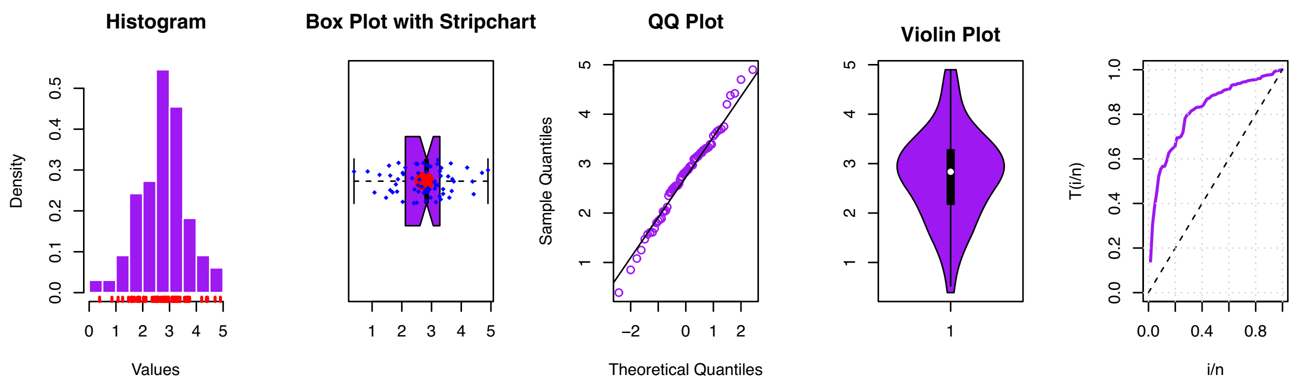

Figure 12: Some basic nonparametric plots for dataset of carbon fibers stress.

{3.15, 1.25, 2.95, 4.38, 2.12, 1.47, 0.39, 2.79, 2.59, 2.05, 2.56, 3.65, 2.74, 1.87, 3.56, 4.42, 3.31, 2.55, 2.03, 3.19, 2.67, 3.22, 2.48, 2.43, 4.70, 3.09, 4.90, 1.61, 3.22, 2.50, 2.93, 3.68, 1.57, 1.80, 2.53, 2.81, 1.84, 2.87, 1.61, 3.11, 2.41, 3.60, 3.75, 3.27, 2.82, 2.35, 2.96, 3.39, 2.55, 0.85, 3.28, 3.11, 2.03, 1.08, 3.27, 2.03, 1.69, 3.39, 2.73, 3.31, 2.88, 4.20, 3.33}.

This dataset allows for deeper analysis into the variability and resilience of carbon fibers under extreme stress conditions. Researchers can apply these data to optimize material performance and design more efficient and durable composites, which are integral to high-stress environments.

In Table 12, we provide an in-depth comparison of various models using MLE with StEr, KSD, PVKS, CVM, PVCVM, AD, and PVAD. Among the tested distributions, the SPB-X distribution consistently outperformed others across multiple metrics, including KSD, PVKS, CVM, PVCVM, AD, and PVAD, making it the most suitable model for breaking stress of carbon fibers dataset.

Figure 12 includes the histogram, violin plot, QQ plot, box plot with stripchart, and TTT plot of dataset of breaking stress of carbon fibers datasets. The estimated PDFs of competing models for the of dataset of breaking stress of carbon fibers datasets are shown in Figure 13, while Figure 14 displays the estimated CDFs of the competitive models. In addition, Figure 15 illustrates the PP plots of the competing models. Figures 13–15 demonstrate the fit of our distribution to the actual data.

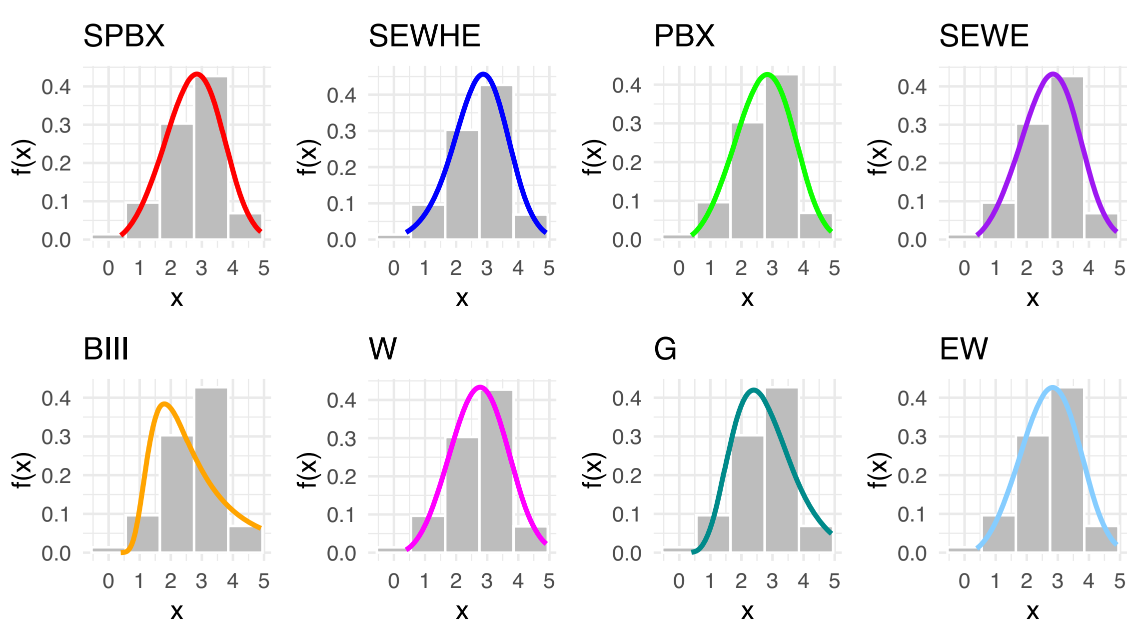

Figure 13: Estimated PDFs for the competing models for dataset of carbon fibers stress.

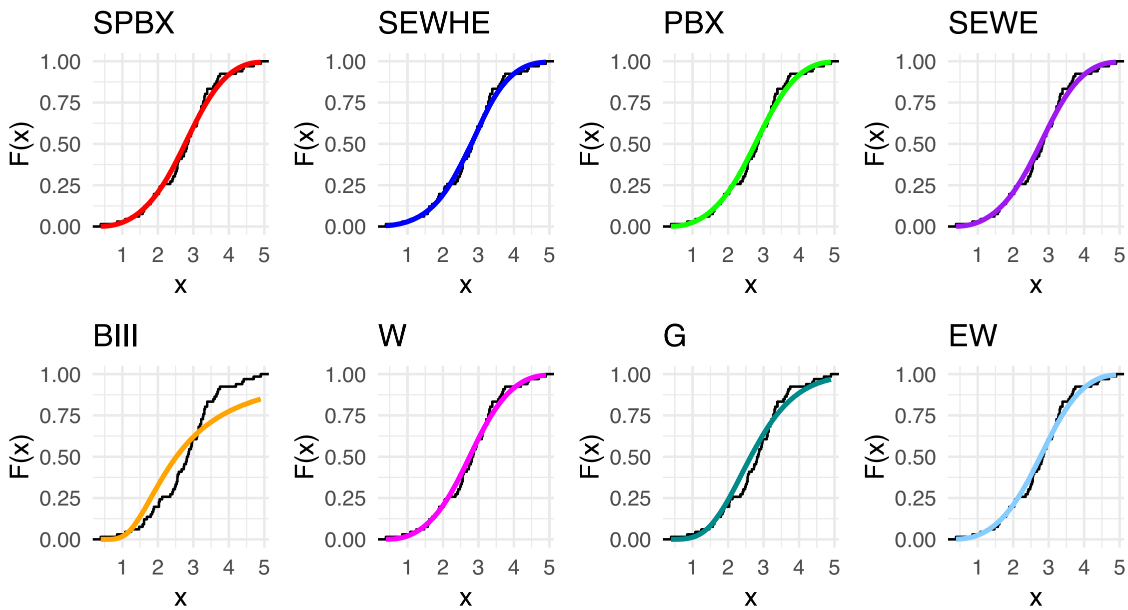

Figure 14: Estimated CDFs for the competing models for dataset of carbon fibers stress.

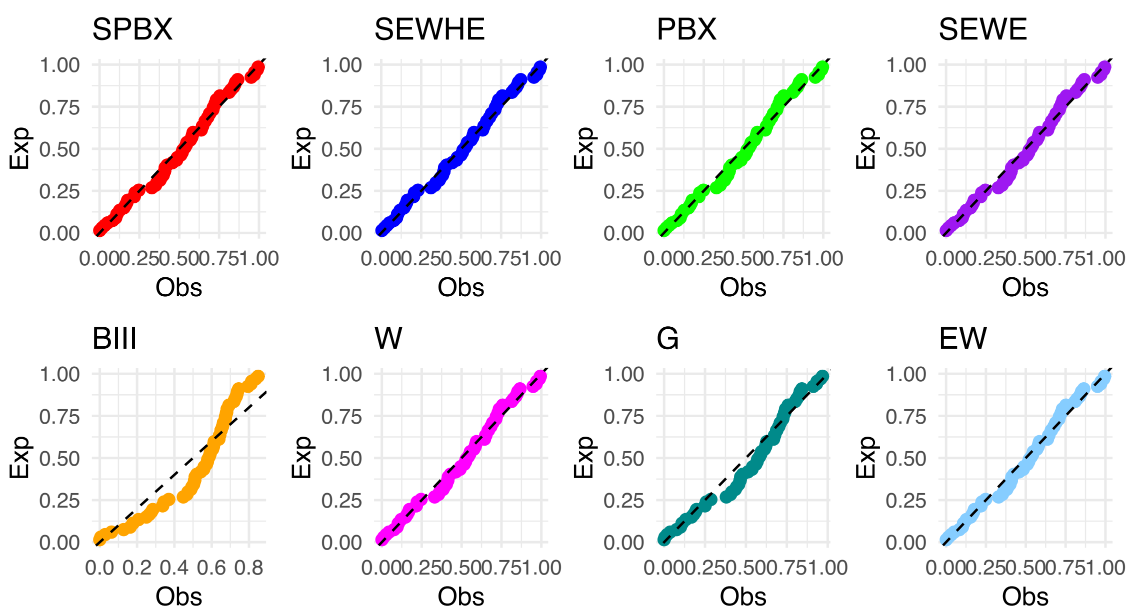

Figure 15: The PP plot for the competing models for dataset of carbon fibers stress.

8.3 Tensile strength of carbon fibers dataset

Tensile strength, typically expressed in Gigapascals (GPa), measures the maximum stress a single carbon fiber can withstand before fracturing under tension. This property is essential in evaluating the performance and reliability of carbon fiber-reinforced materials, widely applied across industries such as aerospace, automotive, and sports equipment manufacturing. An in-depth understanding of the tensile strength of carbon fibers directly influences the design and development of more durable and resilient composite structures.

The dataset used in this study, sourced from Kundu and Raqab [41], contains tensile strength measurements for individual carbon fibers, expressed in GPa. The following is the dataset:

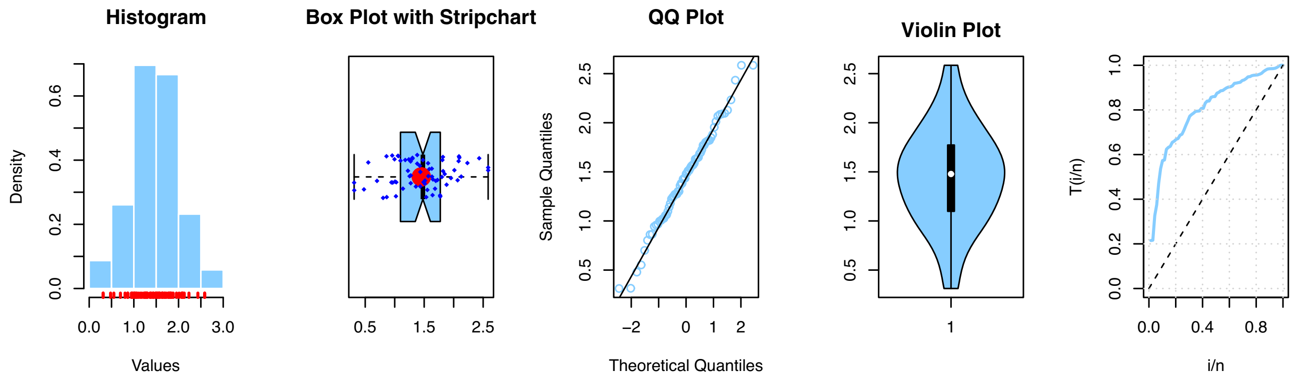

Figure 16: Some basic nonparametric plots for dataset of carbon fibers strength.

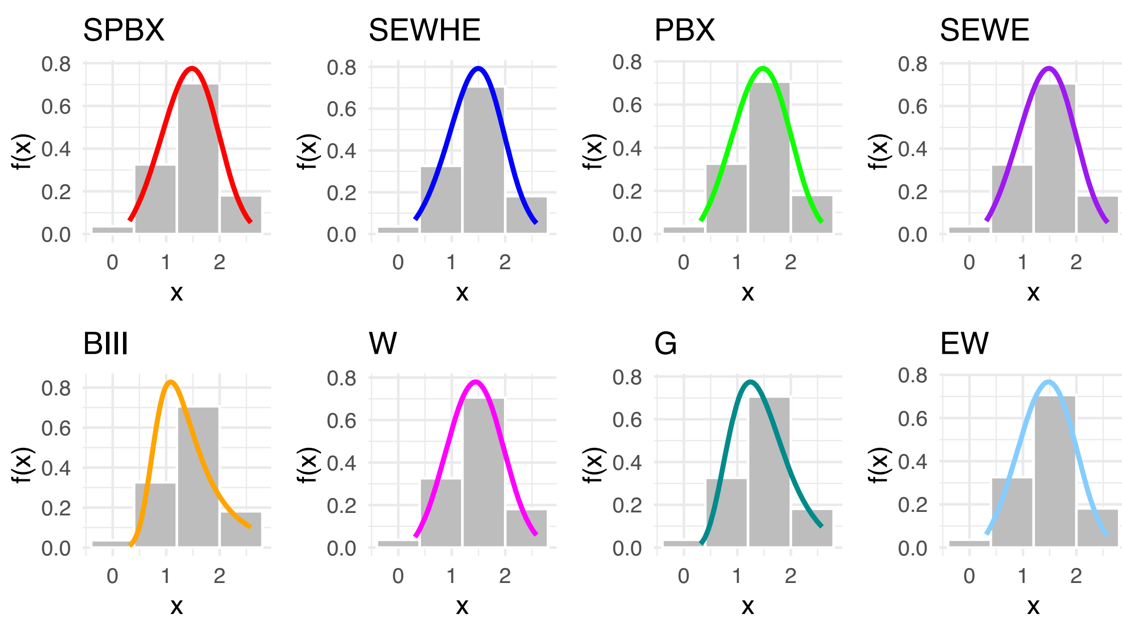

Figure 17: The PDF plot of SPB-X distribution for dataset of carbon fibers strength.

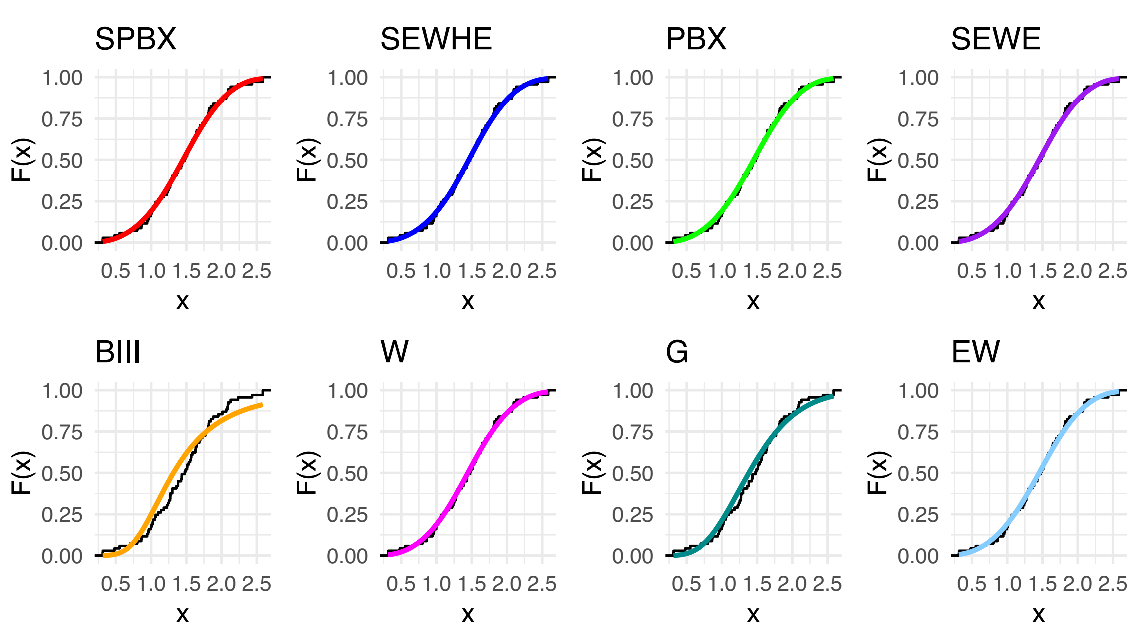

Figure 18: The CDF plot of SPB-X distribution for dataset of carbon fibers strength.

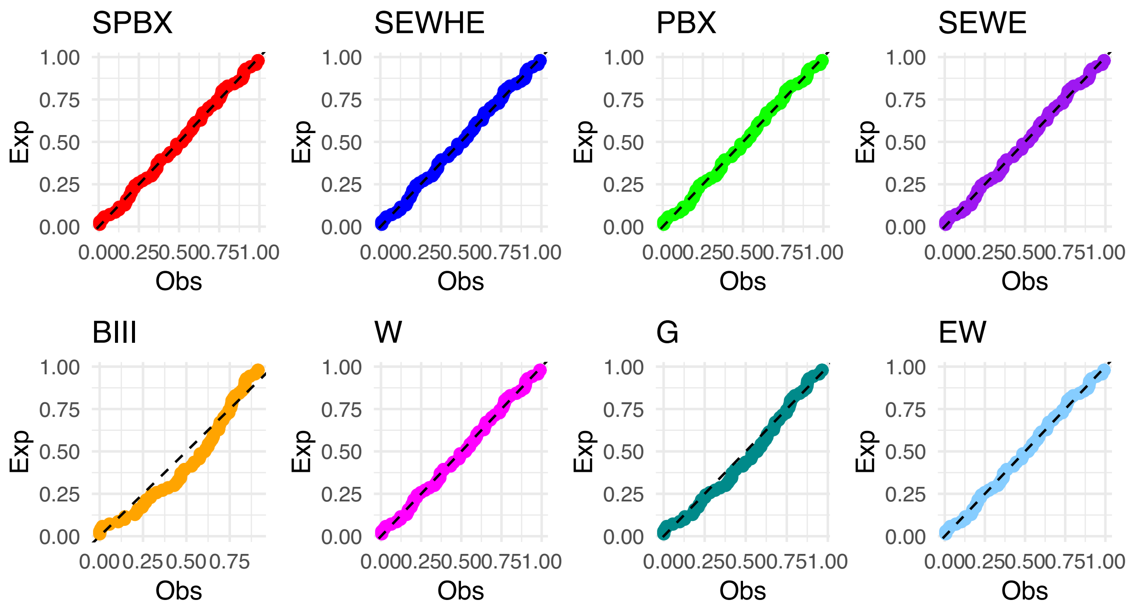

Figure 19: The PP plot of SPB-X distribution for dataset of carbon fibers strength.

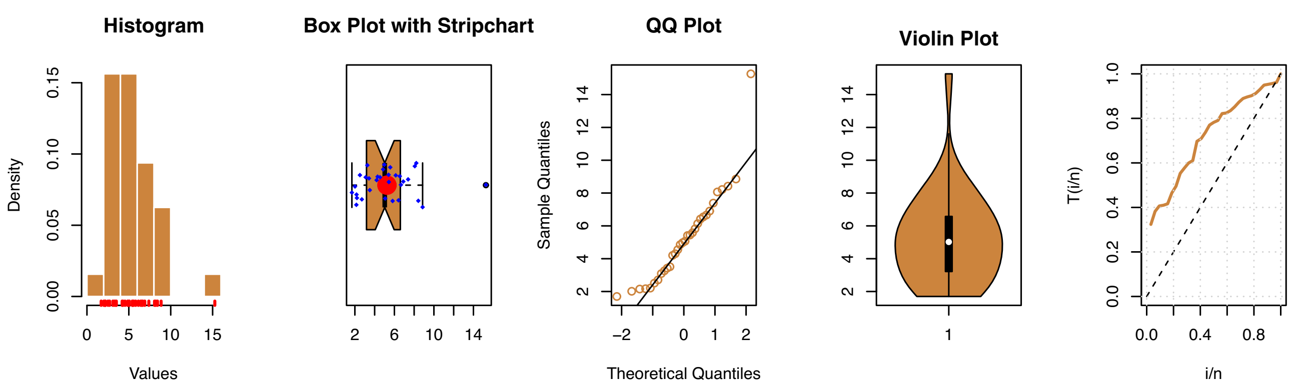

Figure 20: Some basic nonparametric plots for insurance dataset.

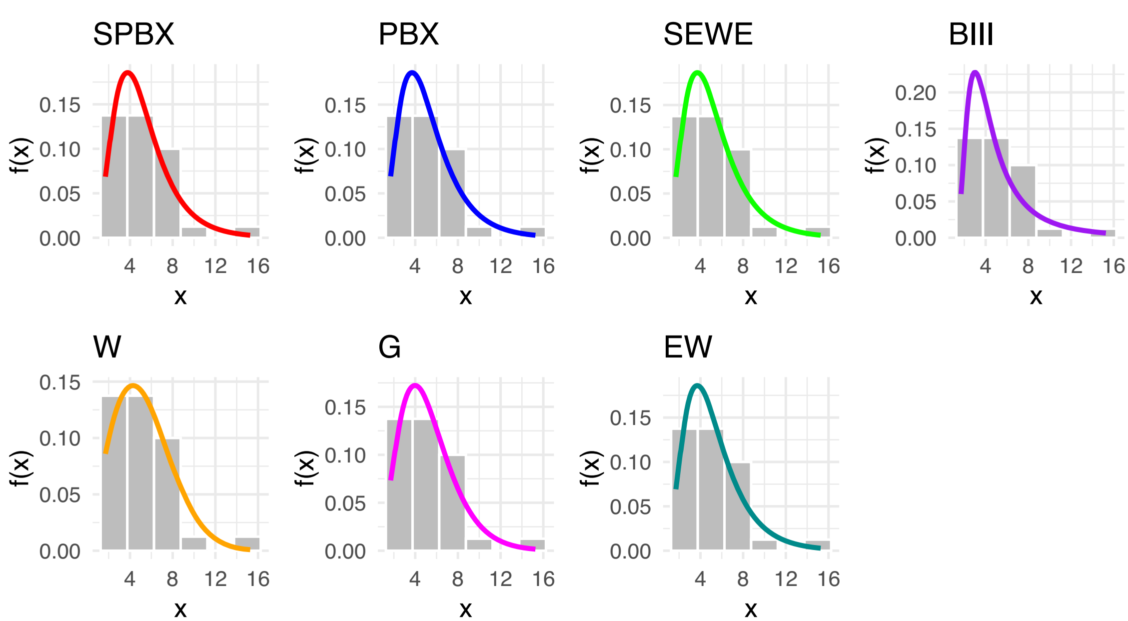

Figure 21: Estimated PDFs for the competing models for insurance dataset.

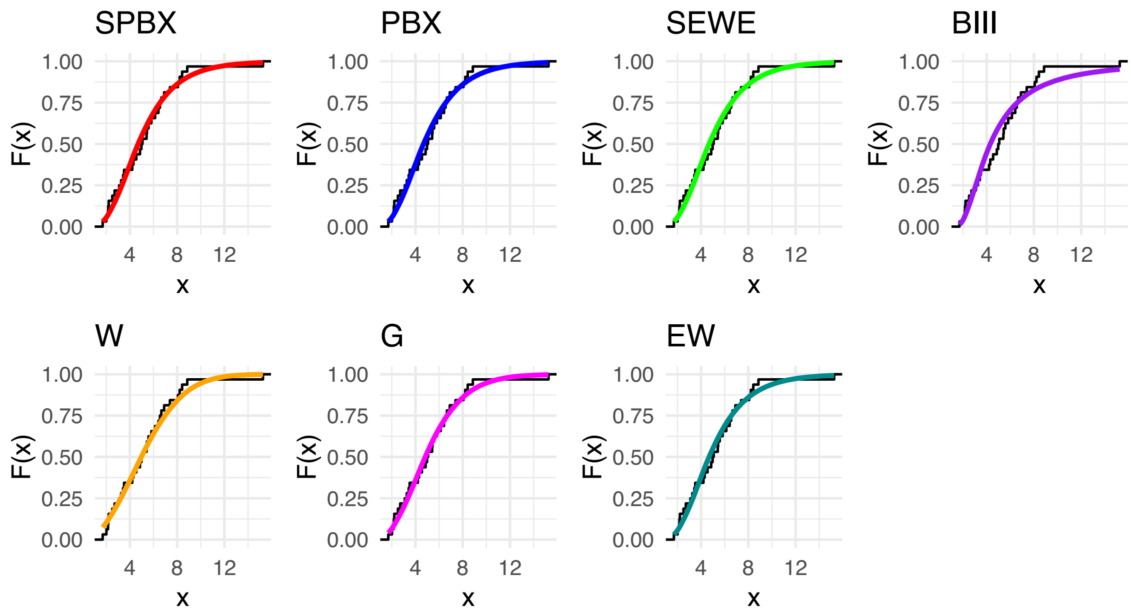

Figure 22: Estimated CDFs for the competing models for insurance dataset.

{1.098, 1.253, 0.944, 1.055, 1.586, 1.773, 1.554, 2.012, 1.301, 1.179, 1.884, 0.966, 0.552, 1.179, 1.642, 0.312, 1.426, 1.726, 0.865, 1.063, 0.803, 1.514, 1.270, 2.233, 1.301, 1.240, 1.627, 2.096, 1.533, 1.534, 1.321, 1.801, 1.559, 0.865, 0.979, 2.094, 1.300, 0.865, 1.434, 1.235, 2.585, 1.684, 2.012, 1.048, 1.373, 1.633, 1.697, 0.753, 1.726, 1.754}.

This dataset provides critical insights into the variability of tensile strength between individual fibers, allowing engineers and materials scientists to optimize the use of carbon fibers in high-performance applications. Using such data, industries can create composites that push the boundaries of durability and functionality in demanding environments.

In Table 13, we provide an in-depth comparison of various models using MLE with StEr, KSD, PVKS, CVM, PVCVM, AD, and PVAD. Among the tested distributions,

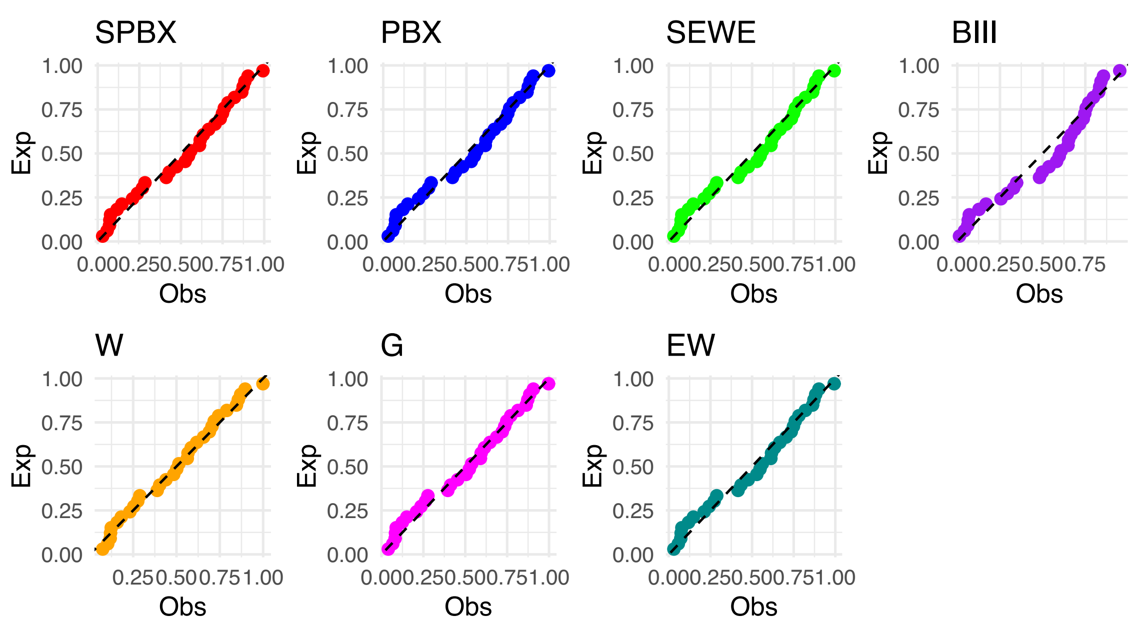

Figure 23: Estimated CDFs for the competing models for insurance dataset.

the SPB-X distribution consistently outperformed others across multiple metrics, including KSD, PVKS, CVM, PVCVM, AD, and PVAD, making it the most suitable model for the tensile strength of the carbon fibers dataset.

Figure 16 includes the histogram, violin plot, QQ plot, box plot with stripchart, and TTT plot of dataset of tensile stress of carbon fibers datasets. The estimated PDFs of competing models for the of dataset of tensile stress of carbon fibers datasets are shown in Figure 17, while Figure 18 displays the estimated CDFs of the competitive models. In addition, Figure 19 illustrates the PP plots of the competing models. Figures 17–19 demonstrate the fit of our distribution to the actual data.

8.4 Insurance dataset

The insurance dataset, which spans the years 1987–2017, displays the excess of assets over liabilities for investments made by insurance companies, pension funds, and trusts. The values are expressed in billions of pounds. The following is the electronic address that it was obtained from: The link https://www.ons.gov.uk/ references the aforementioned product. The dataset is reported in Table 14.

In Table 15, we provide an in-depth comparison of various models using MLE with StEr, KSD, PVKS, CVM, PVCVM, AD, and PVAD. Among the tested distributions, the SPB-X distribution consistently outperformed others

Table 16: The actuarial metrics VaR, ES, TVaR, and TV values for the insurance dataset

Measure	q	SPB-X	PBX	SEWE	Measure	q	SPB-X	PBX	SEWE
VaR	0.650	5.6930	5.6868	5.6815	TVaR	0.650	8.1786	8.1798	8.1864
	0.700	6.0936	6.0942	6.0883		0.700	8.5602	8.5620	8.5707
	0.750	6.5548	6.5636	6.5577		0.750	9.0087	9.0100	9.0215
	0.800	7.1068	7.1253	7.1199		0.800	9.5554	9.5537	9.5695
	0.850	7.8061	7.8351	7.8317		0.850	10.2603	10.2501	10.2728
	0.900	8.7813	8.8196	8.8215		0.900	11.2598	11.2275	11.2621
	0.910	9.0343	9.0736	9.0772		0.910	11.5214	11.4812	11.5193
	0.920	9.3174	9.3569	9.3629		0.920	11.8150	11.7648	11.8070
	0.930	9.6388	9.6776	9.6864		0.930	12.1493	12.0863	12.1336
	0.940	10.0109	10.0474	10.0598		0.940	12.5376	12.4578	12.5112
	0.950	10.4529	10.4843	10.5016		0.950	13.0001	12.8975	12.9586
	0.960	10.9973	11.0190	11.0430		0.960	13.5715	13.4364	13.5076
	0.970	11.7060	11.7088	11.7426		0.970	14.3173	14.1328	14.2184
	0.975	12.1596	12.1465	12.1873		0.975	14.7957	14.5752	14.6705
	0.980	12.7200	12.6832	12.7331		0.980	15.3873	15.1177	15.2255
	0.985	13.4515	13.3766	13.4396		0.985	16.1607	15.8193	15.9443
	0.990	14.5011	14.3577	14.4412		0.990	17.2715	16.8120	16.9634
	0.995	16.3499	16.0457	16.1700		0.995	19.2293	18.5203	18.7222
	0.999	20.9308	20.0204	20.2655		0.999	24.0749	22.5402	22.8827
ES	0.650	3.6882	3.6717	3.0239	TV	0.650	6.2552	5.9357	6.0739
	0.700	3.8454	3.8299	3.1817		0.700	6.2759	5.9001	6.0496
	0.750	4.0103	3.9961	3.3478		0.750	6.3207	5.8717	6.0364
	0.800	4.1860	4.1735	3.5252		0.800	6.4003	5.8557	6.0379
	0.850	4.3774	4.3671	3.7190		0.850	6.5323	5.8534	6.0582
	0.900	4.5932	4.5853	3.9378		0.900	6.7623	5.8743	6.1107
	0.910	4.6406	4.6332	3.9859		0.910	6.8288	5.8828	6.1274
	0.920	4.6898	4.6830	4.0359		0.920	6.9061	5.8936	6.1473
	0.930	4.7413	4.7350	4.0881		0.930	6.9969	5.9070	6.1710
	0.940	4.7953	4.7895	4.1429		0.940	7.1061	5.9239	6.1998
	0.950	4.8525	4.8470	4.2009		0.950	7.2404	5.9453	6.2352
	0.960	4.9135	4.9084	4.2628		0.960	7.4118	5.9739	6.2815
	0.970	4.9797	4.9748	4.3299		0.970	7.6437	6.0116	6.3398
	0.975	5.0153	5.0104	4.3660		0.975	7.7954	6.0358	6.3776
	0.980	5.0532	5.0482	4.4043		0.980	8.1037	6.0678	6.4260
	0.985	5.0938	5.0886	4.4454		0.985	8.2437	6.1081	6.4876
	0.990	5.1385	5.1328	4.4906		0.990	8.6181	6.1666	6.5745
	0.995	5.1897	5.1829	4.5421		0.995	9.2927	6.2645	6.7159
	0.999	5.2410	5.2322	4.5935		0.999	10.9996	6.4753	7.0392

Table 17: The actuarial metrics TVP values for the insurance dataset

ω	q	SPB-X	PBX	SEWE	ω	q	SPB-X	PBX	SEWE
0.50	0.650	11.3062	11.1476	11.2233	0.90	0.650	13.8083	13.5219	13.6528
	0.700	11.6982	11.5121	11.5955		0.700	14.2085	13.8721	14.0153
	0.750	12.1690	11.9459	12.0397		0.750	14.6973	14.2946	14.4543
	0.800	12.7555	12.4815	12.5884		0.800	15.3156	14.8238	15.0036
	0.850	13.5265	13.1768	13.3019		0.850	16.1395	15.5182	15.7251
	0.900	14.6410	14.1646	14.3174		0.900	17.3459	16.5143	16.7617
	0.910	14.9358	14.4226	14.5830		0.910	17.6674	16.7757	17.0340
	0.920	15.2680	14.7116	14.8807		0.920	18.0304	17.0690	17.3396
	0.930	15.6478	15.0398	15.2191		0.930	18.4466	17.4026	17.6875
	0.940	16.0906	15.4197	15.6110		0.940	18.9331	17.7893	18.0910
	0.950	16.6203	15.8702	16.0762		0.950	19.5165	18.2483	18.5702
	0.960	17.2774	16.4234	16.6484		0.960	20.2421	18.8129	19.1610
	0.970	18.1391	17.1386	17.3882		0.970	21.1966	19.5432	19.9242
	0.975	18.6934	17.5931	17.8593		0.975	21.8115	20.0074	20.4103
	0.980	19.4391	18.1517	18.4385		0.980	22.6806	20.5788	21.0089
	0.985	20.2825	18.8733	19.1881		0.985	23.5800	21.3166	21.7831
	0.990	21.5805	19.8953	20.2507		0.990	25.0278	22.3620	22.8805
	0.995	23.8756	21.6525	22.0802		0.995	27.5927	24.1583	24.7666
	0.999	29.5747	25.7779	26.4023		0.999	33.9745	28.3680	29.2180
0.75	0.650	12.8700	12.6316	12.7418	0.99	0.650	14.3712	14.0561	14.1995
	0.700	13.2672	12.9871	13.1079		0.700	14.7734	14.4031	14.5598
	0.750	13.7492	13.4138	13.5488		0.750	15.2661	14.8230	14.9976
	0.800	14.3556	13.9454	14.0979		0.800	15.8916	15.3508	15.5470
	0.850	15.1596	14.6402	14.8164		0.850	16.7274	16.0450	16.2704
	0.900	16.3316	15.6332	15.8451		0.900	17.9545	17.0430	17.3116
	0.910	16.6431	15.8933	16.1149		0.910	18.2820	17.3052	17.5855
	0.920	16.9945	16.1850	16.4175		0.920	18.6520	17.5994	17.8929
	0.930	17.3970	16.5166	16.7619		0.930	19.0763	17.9343	18.2429
	0.940	17.8672	16.9007	17.1610		0.940	19.5726	18.3224	18.6489
	0.950	18.4304	17.3565	17.6350		0.950	20.1681	18.7834	19.1314
	0.960	19.1304	17.9168	18.2187		0.960	20.9092	19.3506	19.7263
	0.970	20.0500	18.6415	18.9732		0.970	21.8845	20.0843	20.4947
	0.975	20.6422	19.1020	19.4537		0.975	22.5131	20.5506	20.9843
	0.980	21.4650	19.6686	20.0450		0.980	23.4099	21.1249	21.5873
	0.985	22.3434	20.4004	20.8100		0.985	24.3219	21.8663	22.3670
	0.990	23.7351	21.4370	21.8943		0.990	25.8034	22.9170	23.4722
	0.995	26.1988	23.2187	23.7592		0.995	28.4290	24.7221	25.3710
	0.999	32.3246	27.3967	28.1621		0.999	34.9645	28.9508	29.8515

across multiple metrics, including KSD, PVKS, CVM, PVCVM, AD, and PVAD, making it the most suitable model for insurance dataset.

Figure 20 includes the histogram, violin plot, QQ plot, box plot with stripchart, and TTT plot of dataset of insurance datasets. The estimated PDFs of competing models for the of dataset of insurance datasets are shown in Figure 21, while Figure 22 displays the estimated CDFs of the competitive models. In addition, Figure 23 illustrates the PP plots of the competing models. Figures 21–23 demonstrate the fit of our distribution to the actual data.

The actuarial measures VaR, ES, TVaR, TV, and TVP of the SPB-X, PBX, and SEWE distributions are computed and compared using the actual dataset in the following. Tables 16 and 17 present the numerical findings.

Figure 24 includes the competing model VaR, ES, TVaR, and TV plots for the insurance dataset. the competing model TVP plots for the insurance dataset shown in Figure 25.

We find that for different significance levels q and different values of ω, the SPB-X model has higher values for the risk measures VaR, ES, TVaR, TV, and TVP from Tables 16 and 17 and Figures 24 and 25. This suggests that compared to the PBX and SEWE distributions, the SPB-X model has a heavier tail.

From Table 18, it is observed that both estimation methods produce consistent results with only minor

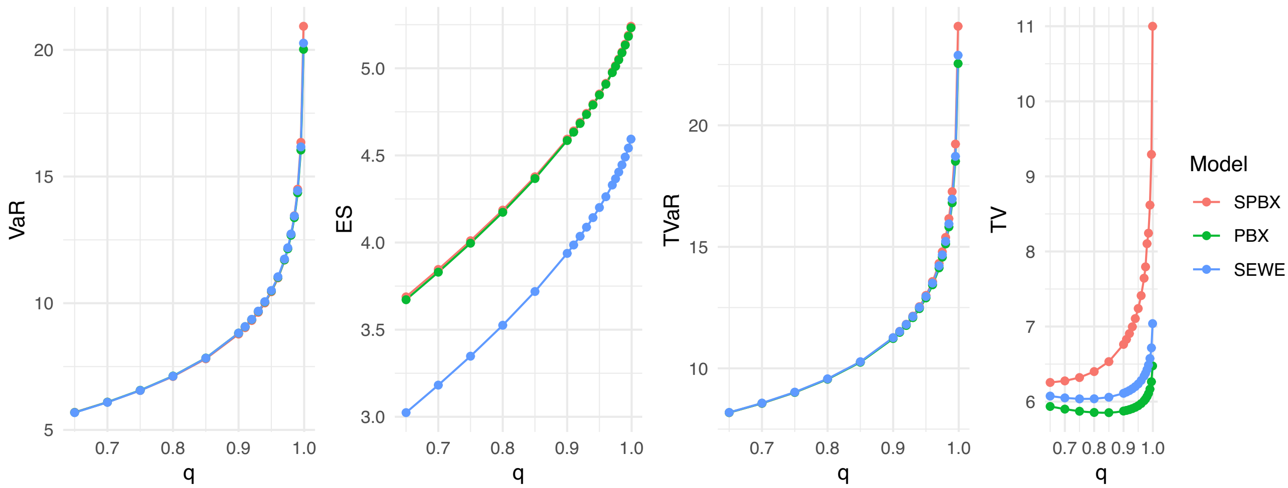

Figure 24: Competing model VaR, ES, TVaR, and TV plots for the insurance dataset.

differences in the estimated parameters. In several datasets (Data1, Data3, Data4, and Data5), LSE achieves slightly smaller KS values and higher p-values compared to MLE, confirming its robustness in certain contexts. However, in other cases (Data2), MLE and LSE results are very close. These findings indicate that while LSE may have some advantages in terms of goodness-of-fit, both methods lead to the same empirical conclusion: the proposed SPB-X distribution provides the best overall fit to the datasets. Thus, the choice of estimation method does not alter the validity of the application results reported in Section 8.

Table 18: Parameter estimates of the SPB-X distribution using MLE and LSE for the five datasets, along with KSD and PVKS

Data	Method	α	θ	λ	KSD	PVKS
Data1	**MLE**	14.5195	0.8207	1.0578	0.1684	0.9141
	LSE	19.8840	1.0673	0.7378	0.1415	0.9803
Data2	**MLE**	2.7126	0.2305	1.0543	0.1036	0.9978
	LSE	1.7772	0.1973	1.0428	0.1088	0.9957
Data3	**MLE**	0.8472	0.0878	1.8287	0.0784	0.8124
	LSE	0.5967	0.0255	2.7033	0.0616	0.9635
Data4	**MLE**	0.8548	0.2995	1.7155	0.0470	0.9980
	LSE	1.0035	0.3514	1.5885	0.0386	0.9999
Data5	**MLE**	16.8042	1.0771	0.2799	0.0881	0.9463
	LSE	0.6613	0.0505	1.3798	0.0791	0.9787

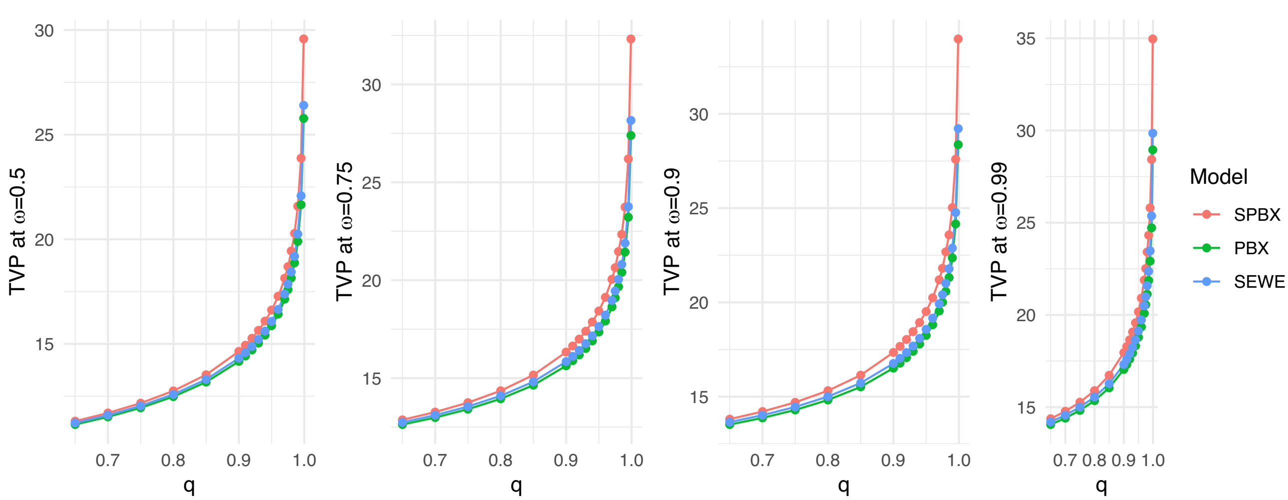

Figure 25: Competing model TVP plots for the insurance dataset.

9 Concluding remarks

In this article, we discuss a novel three-parameter lifespan distribution known as the sine power Burr X (SPB-X) distribution. The suggested distribution is derived from the sine-G class of distributions and the power Burr-X distribution. The suggested distribution encompasses several features, including explicit formulations for the quantile function, Bowley skewness, Moors kurtosis, ordinary moments, generating function, and incomplete and conditional moments, with several numerical and graphical representations. Several notable reliability measures for the SPB-X model include standard reliability functions, mean residual life function, mean waiting time function, residual moment, and inverted residual life. Several critical risk metrics for the SPB-X distribution. Risk measurements include the value at risk, projected shortfall, TVaR, TV, and TVP. Four estimation strategies were used to determine the model parameters: maximum likelihood, least squares, MPS, and Bayesian. A simulation study is conducted to evaluate the efficacy of estimating techniques. Ultimately, five actual datasets are examined to assess the utility and adaptability of the suggested approach. The limitation of this article lies in estimating the parameters of the SPB-X model using the complete samples only. This reason opens the door for future studies to study the estimation of the parameters of the new distribution using different censored schemes for the censored data.

Funding information: This work was supported and funded by the Deanship of Scientific Research at Imam Mohammad Ibn Saud Islamic University (IMSIU) (grant number IMSIU-DDRSP2502).

Author contribution: All authors have accepted responsibility for the entire content of this manuscript and approved its submission.

Conflict of interest: The authors state no conflict of interest.

Data availability statement: The data that support the findings of this study are available on request from the corresponding author. The data are not publicly available due to privacy or ethical restrictions.

References

[1] Eugene N, Lee C, Famoye F. Beta-normal distribution and its applications. Commun Stat Theory Methods. 2002;31(4):497–512.

[2] Cordeiro GM, de Castro M. A new family of generalized distributions. J Stat Comput Simulat. 2011;81(7):883–98.

[3] Alzaatreh A, Lee C, Famoye F. A new method for generating families of continuous distributions. Metron. 2013;71:63–79.

[4] Hassan AS, Elgarhy M, Shakil M. Type II half-Logistic family of distributions with applications. Pakistan J Stat Operat Res. 2017;13(2):245–64.

[5] Al-Marzouki S, Jamal F, Chesneau Ch, Elgarhy M. Topp-Leone odd Fréchet generated family of distributions with applications to COVID-19 data sets. Comput Model Eng Sci. 2020;125(1):437–58.

[6] Kumar D, Singh U, Singh SK. A new distribution using sine function its application to bladder cancer patients data. J Stat Appl Pro. 2015;4(3):417–27.

[7] Souza L, Junior WRO, de Brito CCR, Chesneau C, Ferreira TAE, Soares L. Generalproperties for the Cos-G class of distributions with applications. Eurasian Bull Math. 2019;2:63–79.

[8] Chesneau C, Jamal F The sine Kumaraswamy-G family of distributions. J Math Ext. 2021;15:1–33.

[9] Al-Babtain AA, Elbatal I, Chesneau C, Elgarhy M. Sine Topp-Leone-G family of distributions: theory and applications. Open Phys. 2020;18:574–93.

[10] Souza L, Junior WRO, de Brito CCR, Chesneau C, Ferreira TAE, Fernandes LR. Tan-G class of trigonometric distributions and its applications. Cubo. 2021;23:1–20.

[11] Wenjing H, Afify Z, Goual H. The arcsine exponentiated-X family: validation andinsurance application. Complexity. 2020;2020:1–18.

[12] Burr IW. Cumulative frequency functions. Ann Math Stat. 1942;13(2):215–32.

[13] Raqab MZ, Kundu D. Burr type X distribution: Revisited. J Probabil Stat Sci. 2006;4:179–93.

[14] Surles JG, Padgett WJ. Inference for reliability and stress-strength for a scaled Burr type X distribution. Lifetime Data Anal. 2001;7:187–200.

[15] Algarni A, Almarashi AM, Elbatal I, Hassan AS, Almetwally EM, Daghistani AM, et al. Type I half logistic Burr XG family: Properties, Bayesian, and non-Bayesian estimation under censored samples and applications to COVID-19 data. Math Problems Eng. 2021;2021:5461130.

[16] Abonongo J, Mwaniki IJ, Aduda JA. Cosine Fréchet loss distribution: properties, actuarial measures and insurance applications. Comput J Math Stat Sci. 2024;3(1):1–32.

[17] Bantan RAR, Chesneau C, Jamal F, Elbatal I, Elgarhy M. The truncated Burr X-G family of distributions: Properties and applications to actuarial and financial data. Entropy 2021;23:1088.

[18] Suleiman AA, Daud H, Singh NSS, Ishaq AI, Othman M. A new odd beta prime-Burr X distribution with applications to petroleum rock sample data and COVID-19 mortality rate. Data. 2023;8:143.

[19] Soliman D, Hegazy MA, AL-Dayian GR, EL-Helbawy AA. Statistical properties and applications of a new truncated Zubair-generalized family of distributions. Comput J Math Stat Sci. 2025;4(1):222–57.

[20] Khan MS, King R, Hudson IL. Transmuted Burr type X distribution with covariates regression modeling to analyze reliability data. Am J Math Manag Sci. 2020;39:99–121.

[21] Elbatal IA, Helal TS, Elsehetry AM, Elshaarawy RS. Topp-Leone Weibull generated family of distributions with applications. J Business Environ Sci. 2022;1(1):183–95. doi: 10.21608/jcese.2022.270143.

[22] Usman RM, Ilyas M. The power Burr Type X distribution: Properties, regression modeling and applications. Punjab Univ J Math. 2020;52:27–44.
[23] Butt NS, Khalil MG. A new bimodal distribution for modeling asymmetric bimodal heavy- tail real lifetime data. Symmetry. 2020;12:2058.
[24] Usman RM, Handique L, Chakraborty S. Some aspects of the odd log-logistic Burr X distribution with applications in reliability data modeling. Int J Appl Math Stat. 2019;58:127–47.
[25] Shrahili M, Elbatal M, Muhammad M. The type I half-logistic Burr X distribution: Theory and practice. J Nonlinear Sci Appl 2019;12:262–77.
[26] Abdullah ZM, Khaleel MA, Abdal-hameed MK, Oguntunde PE. Estimating parameters for extension of Burr type X distribution by using conjugate gradient in unconstrained optimization. Kirkuk Univ. 2019;14:33–49.
[27] Khaleel MA, Ibrahim NA, Shitan M, Merovci F. New extension of Burr type X distribution properties with application. J King Saud Univ Sci. 2018;30(4):450–7.
[28] Madaki UY, Abu Bakar MR, Handique L. Beta Kumaraswamy Burr type X distribution and its properties. Preprints 2018;2018080356.
[29] Ishaq A, Usman A, Tasi'u M, Aliyu Y. Weibull-Burr type x distribution: Its properties and application. Niger. 2017;16:150–7.
[30] Al-Saiari AY, Baharith LA, Mousa SA. New extended burr type X distribution. Sri Lankan J Appl Stat. 2016;17:217–31.
[31] Khaleel MA, Ibrahim NA, Shitan M, Merovci F. Some properties of Gamma Burr type X distribution with application. In Proceedings of the AIP Conference Proceedings, Yogyakarta, Indonesia, 25–26 January 2016; p. 020087.
[32] Merovci F, Khaleel MA, Ibrahim NA, Shitan M. The beta Burr type X distribution properties with application. SpringerPlus. 2016;5:697.
[33] Hassan OHM, Elbatal I, Al-Nefaie AH, Elgarhy M. On the Kavya-Manoharan-Burr X model: estimations under ranked set sampling and applications. J Risk Financial Manag. 2023;16:19.
[34] Kenney FJ, Keeping SE. Mathematics of statistics. NJ: Princeton; 1962.
[35] Moors AJ. A quantile alternative for Kurtosis. J R Stat Soc D. 1998;37:25–32.
[36] Artzner P. Application of coherent risk measures to capital requirements in insurance. North Am Actuarial J. 1999;3(2):11–25.
[37] Artzner P, Delbaen F, Eber J-M, Heath D. Thinking coherently. Risk. 1997;10(11):14.
[38] Artzner P, Delbaen F, Eber J-M, Heath D. Coherent measures of risk. Math Fin. 1999;9(3):203–28.
[39] Landsman Z. On the tail mean-variance optimal portfolio selection. Insur Math Econ. 2010;46:547–53.
[40] Cordeiro GM, Lemonte AJ. The β-Birnbaum-Saunders distribution: An improved distribution for fatigue life modeling. Comput Stat Data Anal. 2011;55(3):1445–61.
[41] Kundu D, Raqab MZ. Estimation of $R = P(Y < X)$ for three-parameter Weibull distribution. Stat Probab Lett. 2009;79(17):1839–46.
[42] Alyami SA, Elbatal I, Alotaibi N, Almetwally EM, Elgarhy M. Modeling to factor productivity of the United Kingdom food Chain: using a new lifetime-generated family of distributions. Sustainability. 2022;14(14):8942.
[43] Shah A, Gokhale DV. On maximum product of spagings (mps) estimation for burr xii distributions: On maximum product of spagings. Commun Stat-Simulat Comput. 1993;22(3):615–41.
[44] Shao Y, Hahn MG. Maximum product of spacings method: A unified formulation with illustration of strong consistency. Illinois J Math. 1999;43(3):489–99.
[45] Husain QN, Qaddoori AS, Noori NA, Abdullah KN, Suleiman AA, Balogun OS. New expansion of Chen distribution according to the nitrosophic logic using the Gompertz family. Innovat Stat Probab. 2025;1(1):60–75.
[46] Noori NA, Khaleel MA, Khalaf SA, Dutta S. Analytical modeling of expansion for odd Lomax generalized exponential distribution in framework of neutrosophic logic: a theoretical and applied on neutrosophic data. Innovat Stat Probab. 2025;1(1):47–59. doi: 10.64389/isp.2025.01104.
[47] Onyekwere CK, Aguwa OC, Obulezi OJ. An updated lindley distribution: properties, estimation, acceptance sampling, actuarial risk assessment and applications. Innovat Stat Probab. 2025;1(1):1–27. doi: 10.64389/isp.2025.01103.
[48] Gemeay AM, Moakofi T, Balogun OS, Ozkan E, Hossain MM. Analyzing real data by a new heavy-tailed statistical model. Modern J Stat. 2025;1(1):1–24. doi: 10.64389/mjs.2025.01108.
[49] Sapkota LP, Kumar V, Tekle G, Alrweili H, Mustafa MS, Yusuf M. Fitting real data sets by a new version of Gompertz distribution. Modern J Stat. 2025;1(1):25–48. doi: 10.64389/mjs.2025.01109.
[50] El-Sherpieny ESA, Almetwally EM, Muhammed HZ. Progressive type-II hybrid censored schemes based on maximum product spacing with application to power Lomax distribution. Phys A Stat Mech Appl. 2020;553:124251.
[51] Alshenawy R, Sabry MA, Almetwally EM, Almongy HM. Product spacing of stress-strength under progressive hybrid censored for exponentiated-gumbel distribution. Comput Materials Continua. 2021;66(3):2973–95.
[52] Weibull W. A: statistical distribution function of wide applicability. J Appl Mech. 1951;18:293–7. doi: 10.1115/1.4010337.
[53] Thom HC. A note on the gamma distribution. Monthly Weather Rev. 1958;86(4):117–22.
[54] Nadarajah S, Cordeiro GM, Ortega EM. The exponentiated Weibull distribution: a survey. Stat Papers. 2013;54:839–77.
[55] Cordeiro GM, Gomes AE, da-Silva CQ, Ortega EM. A useful extension of the Burr III distribution. J Stat Distributions Appl. 2017;4:1–15.
[56] Lim JT, Azizan AS. Weather and climate of Malaysia. Kuala Lumpur: University of Malaya Press; 2004.
[57] Ruzhansky M, Cho YJ, Agarwal P, Area I (Eds.). Advances in real and complex analysis with applications. Singapore: Springer; 2017.
[58] Butt SI, Sayyari Y, Agarwal P, Nieto JJ, Umar M. On some inequalities for uniformly convex mapping with estimations to normal distributions. J Inequal Appl. 2023;2023: 89. doi: 10.1186/s13660-023-02997-z.
[59] Tierney L. Markov chains for exploring posterior distributions. Ann Stat. 1994;22(4):1701–28.
[60] Suhaila J, Sayang MD, Jemain AA. Revised spatial weighting methods for estimation of missing rainfall data. Asia Pac J Atmos Sci. 2008;44:93–104.
[61] Wijngaard JB, Klein Tank AMG, Konnen GP. Homogeneity of 20th century European daily temperature and precipitation series. Int J Climatol 2003;23:679–92.
[62] Suhaila J, Deni SM, Wan Zin WZ, Jemain AA. Spatial patterns and trends of daily rainfall regime in Peninsular Malaysia during the southwest and northeast monsoons: 1975–2004. Meteorol Atmos Phys. 2010;110:1–18.